Atmos. Chem. Phys. Discuss., 15, 23841–23891, 2015
www.atmos-chem-phys-discuss.net/15/23841/2015/
doi:10.5194/acpd-15-23841-2015

Atmospheric Chemistry and Physics Discussions

Characterizing tropospheric ozone and CO around Frankfurt between 1994–2012 based on MOZAIC-IAGOS aircraft measurements

H. Petetin, V. Thouret, A. Fontaine, B. Sauvage, G. Athier, R. Blot, D. Boulanger, J.-M. Cousin, and P. Nedelec

CNRS and Université Paul Sabatier, Laboratoire d'Aérologie, Toulouse, France

Received: 8 July 2015 – Accepted: 14 August 2015 – Published: 3 September 2015

Correspondence to: H. Petetin (herve.petetin@aero.obs-mip.fr)

Published by Copernicus Publications on behalf of the European Geosciences Union.

Abstract

In the framework of the MOZAIC-IAGOS program, ozone and carbon monoxide vertical profiles are available since 1994 and 2002, respectively. This study investigates the variability and trends of both species at several tropospheric layers above the Frankfurt and Munich airports where about 21 600 flights have been performed over the 1994–2012 period, which represents the densest dataset in the world (about 75 flights per month on average). Over that period, most mean ozone trends are positive but insignificant at a 95 % confidence level, except in winter where significant upward trends (around $+0.38 \pm 0.24$ ppb yr^{-1}) are found. Conversely, a significant increase of annual background ozone is highlighted, mostly during winter and autumn. Mean annual ozone trends increase with altitude, the largest increase being found in summer due to a noticeable decrease of highest ozone concentrations observed in the lower troposphere during the second half period. Over the 2002–2012 period, most mean CO trends are significantly negative, the decrease being higher in the lower troposphere compared to the mid- and upper troposphere with again, major differences in summer. Trends in the ozone seasonal cycle are also investigated, with a focus on the phase. Ozone maxima occur earlier and earlier with a shift around -10.6 ± 2.9 days decade^{-1} in the lower troposphere, in agreement with previous studies. The analysis of other ozone datasets in Europe (including surface stations and ozone soundings) confirms this trend, but highlights strong heterogeneities in the phase change. Interestingly, this shift is shown to decrease with altitude, with trends of -4.3 ± 2.4 and -2.0 ± 1.7 days decade^{-1} in the mid- and upper troposphere, respectively. The geographic origin of the air masses sampled by aircraft is analysed with FLEXPART backward simulations and suggests, together with trends and phase changes results, that an increase of the Asian contribution to ozone in the upper troposphere may compensate during summer the decrease of European and North American contributions associated to emission control over these two regions.

ACPD
15, 23841–23891, 2015

1 Introduction

As one of the major sources of hydroxyl radicals (OH) that directly control the atmospheric lifetime of a large number of compounds, ozone plays a unique role in the oxydative capacity of the atmosphere. In the troposphere, it acts as a powerfull greenhouse gas with a positive radiative forcing (RF) of $0.40 \pm 0.20\,\mathrm{W\,m^{-2}}$ that is not compensated by the RF of stratospheric ozone estimated at $-0.05 \pm 0.10\,\mathrm{W\,m^{-2}}$ (IPCC, 2013). It also has well-kown adverse impacts on human health (Jerrett et al., 2009), vegetation (Ashmore, 2005; Paoletti, 2006) and agricultural crop yields (Van Dingenen et al., 2009).

Despite the considerable scientific achievements made during the last decades, the ozone budget remains difficult to quantify precisely, as attested at the global scale by the significant discrepancies from one model to the other, around a factor of 2 for the global ozone production (Wu et al., 2007). In the troposphere, a myriad of anthropogenic and natural precursors is implicated in the photochemical formation of ozone, including methane (CH_4), carbon monoxide (CO), nitrogen oxides (NO_x) and non-methane volatile organic compounds (NMVOC). Intrusions from the stratospheric reservoir represent the other noticeable source of ozone in troposphere (Holton et al., 1995; Stohl et al., 2003b; Zbinden et al., 2006). Conversely, several sinks are at stake in the troposphere, including the photolytic destruction (that leads to OH formation), the dry deposition at ground and the reactive uptake on aerosols (Moise and Rudich, 2000, 2002). Major uncertainties in the simulation of ozone appear related to lightning NO_x production, isoprene biogenic emissions and degradation chemistry, biomass burning emissions, water vapor concentrations and stratosphere–troposphere exchanges (Stevenson et al., 2006). Besides the high variability – both in space and time – of these sources and sinks, the ozone lifetime in troposphere (from days to weeks) appears high enough to allow its advection over long distances, fueling a substancial background at the regional to hemispheric scale (Derwent et al., 2004, 2007; Sudo and Akimoto, 2007). This leads to a large heterogeneity of ozone abundance and vari-

ACPD
15, 23841–23891, 2015

ability in the troposphere, making it difficult to draw a simple and global picture of the ozone present-day concentrations and trends.

During the last decades, ozone trends in free troposphere have been intensively investigated, notably based on ozonesonde long-term observations. Specifically in Europe where such measurements are available over a few decades at several sites (e.g. Hohenpeissenberg, Payerne, Uccle, De Bilt, Legionowo, Lindenberg), most results indicate an increase of ozone levels from the 1960s until the mid-1980s (Logan et al., 1999; Oltmans et al., 1998; Tiao et al., 1986), the only site with no significant trend being Lindenberg, Germany, for the 1975–1983 period (Tiao et al., 1986). Such positive trends were found all along the year without any significant seasonal influence (Logan et al., 1999) and through the entire tropospheric column (Logan et al., 1999; Oltmans et al., 1998). By the mid-1980s until 2000s, most ozonesonde observations in Europe indicate a progressive leveling-off of ozone concentrations in free troposphere (Logan et al., 1999; Oltmans et al., 1998, 2006). For instance, the significant positive trends obtained at Hohenpeissenberg in the entire tropospheric column for 1971–2010 vanish in most tropospheric sublayers considering the 1981–2010 period (Oltmans et al., 2013). Ozone observations at Jungfraujoch, Switzerland (3850 m), an evelated alpine site supposed to be representative of the free troposphere, indeed reveal that concentrations have continued to increase in the 1990s, in particular during winter, the leveling-off occuring only in the 2000s (Cui et al., 2011), as well as ozone levels measured by MOZAIC (Measurements of OZone and water vapour by Airbus In-service airCraft) aircraft above some European airports (Logan et al., 2012). A similar evolution is reported by Cooper et al. (2014) at other mountain or remote sites in Europe.

A full understanding of the ozone variability would ideally require to discriminate and quantify all the ozone budget terms. This can be easily achieved with determinist numerical models, but the confidence in results remains limited by the high uncertainties at stake in both models and input data. An alternative but more qualitative approach consists in taking benefit from the different seasonal patterns of the various ozone budget terms (e.g. precursors emissions, photochemical production, stratospheric in-

ACPD
15, 23841–23891, 2015

trusions, transport regimes) and aims at linking the evolution of ozone seasonality to changes in the contribution of its various sources and sinks. At the Mace Head coastal site during the 1987–2003 period, Simmonds et al. (2004) found the highest ozone increase in both polluted continental (coming from Europe) and baseline (coming from the Atlantic Ocean) air masses during winter while baseline ozone levels increased noticeably less in summer, and do not show any significant trend in polluted air masses. Extending the analysis to the 1988–2012 period, Derwent et al. (2013) noticed that the still increasing baseline ozone levels do not extend to the European ozone load that levelled-off during the 2000s. These results thus suggest a possible compensation between a decrease of ozone local formation in Europe and an increase of ozone imports. At several remote or alpine sites in northern midlatitudes, Parrish et al. (2013) recently highlighted a noticeable shift in the ozone cycle at ground, the maximum daily ozone occuring between 3 and 6 days earlier each decade since the 1970s. Such a shift may reflect some changes in the contributions of the various ozone sources and sinks, e.g. transport pathways, precursors emissions, photochemistry or climate change impacts (Parrish et al., 2013). The present study aims at investigating changes in the variability and seasonality of tropospheric ozone in Central/Western Europe. Based on vertical profiles measured by commercial aircraft implicated in the MOZAIC-IAGOS (In-service Aircraft for a Global Observing System) program, it will focus on the free and upper troposphere in order to go beyond the more limited representativeness of measurements in the boundary layer measurements (close to precursors emissions and/or deposition sink) at the regional scale. However, results in boundary layer will be also presented to give a full picture of the troposphere.

This study will also investigate the variability and trends of carbon monoxide, the other chemical compound measured in the framework of the MOZAIC-IAGOS program. As a long lifetime (several weeks to several months) compound emitted by incomplete combustion processes, carbon monoxide represents an interesting pollution tracer able to provide useful informations on long-range transport at the hemispheric scale. Char-

ACPD
15, 23841–23891, 2015

acterizing carbon monoxide in troposphere may thus help investigating the variability and trends affecting ozone.

Section 2 presents the MOZAIC-IAGOS dataset used in this paper and describes the treatment applied on vertical profile data. Ozone and carbon monoxide variability and trends are analysed in Sect. 3, while long-range transport is investigated in Sect. 4. Results are finally discussed in Sect. 5.

2 Data and methodology

2.1 MOZAIC-IAGOS dataset

In the framework of the MOZAIC-IAGOS program (www.iagos.fr), ozone and carbon monoxide measurements (among other parameters) are performed by commercial aircraft along various trajectories in the world (most of them from or to European airports) since 1994 and 2002, respectively. Until October 2014 (date of the last MOZAIC aircraft flight), both ozone and carbon monoxide have been measured using the same instruments in all aircraft, thus ensuring the dataset consistency during most of the period. Ozone measurements were performed using a dual-beam UV-absorption monitor (time resolution of 4 seconds) with an accuracy estimated at about ±2 ppbv/±2 % (Thouret et al., 1998). Carbon monoxide was measured by an improved infrared filter correlation instrument (time resolution of 30 seconds) with a precision estimated at ±5 ppbv/±5 % (Nedelec et al., 2003). Note also that comparisons between the MOZAIC ozone dataset and other types of data (e.g. mountain surface stations, ozonesonde) have been performed in Europe, showing a good consistency (Logan et al., 2012).

As MOZAIC aircraft have been retired from service, the European partners involved prepared since years the technical successor in the framework of the European Commission (EC) funded IAGOS program. A new concept of aircraft system and instruments has been developed and installed on Airbus long-range aircraft (A340 or A330), starting from July 2011. Six aircraft are actually in operation with IAGOS systems.

ACPD
15, 23841–23891, 2015

The new IAGOS instrumentation is extensively described in Nédélec et al. (2015). Briefly, the O_3 and CO measurements are based on the same technology used for MOZAIC, with the same estimated accuracy and the same data quality control. The nearly 4 years overlap of "old" MOZAIC and "new" IAGOS systems operations allowed to prove that new IAGOS systems provide the same data quality, which is especially important for trends analysis.

The present study will focus on the Frankfurt airport where the longest (from 1994 to 2012) and densest (18 945 flights) record is available. In order to fill a large data gap in 2005, this dataset is combined to data from the Munich airport (2703 flights, mostly between 2002 and 2005), approximately 300 km south-east from Frankfurt, as done in several previous studies (Logan et al., 2012; Zbinden et al., 2006, 2013). Note also that no measurements are available during a part of 2010 due to instrumental problems. An illustration of the dataset density by month and year is shown in Fig. S1 and S2 in the Supplement.

2.2 Tropopause altitude and tropospheric sublayers

This paper focuses on the analysis of tropospheric vertical profiles obtained over Europe (Germany) during both ascent and descent. As tropospheric air masses are subject to very different constraints depending on their altitude (e.g. distance from surface emissions or stratosphere), the troposphere is divided here in three sublayers: the lower troposphere (LT), the mid-troposphere (MT) and the upper troposphere (UT). The UT is defined here as the 60 hPa-width layer below tropopause plus 15 hPa, as in Thouret et al. (2006). The MT is delimited by the UT lower boundary and an arbitrarily fixed altitude of 2 km. Data collected in the 1–2 km layer are finally assigned to the LT, the first kilometer above surface being ignored to limit the representativeness degradation induced by emissions over the airport area (confirmed by significant enhancements of CO concentrations near the ground in most vertical profiles).

The tropopause altitude can be estimated by several approaches, e.g. thermal, dynamic, chemical criteria (Thouret et al., 2006) or a combination of them (Stohl et al.,

ACPD
15, 23841–23891, 2015

2003b). In this paper, tropopause is considered in its dynamic sense, its altitude corresponding to the location at which the potential vorticity (PV) exceeds 2 pvu (1 pvu = 10^{-6} K m^2 kg^{-1} s^{-1}) (see the tropopause height over the 1994–2012 period in Fig. S3 in the Supplement). It is worthwhile keeping in mind that some uncertainties arise from this choice of method, the ozone criteria giving most of time lower dynamical tropopause (DT) compared to the thermal method (Bethan et al., 1996). Two parameters, PV and pressure at which PV reaches 2 pvu (so-called $p_{PV=2}$), are derived along all MOZAIC flights trajectories based on European Centre for Medium-Range Weather Forecasts (ECMWF) operational analysis (00:00, 06:00, 12:00, 18:00 UTC) and forecasts (03:00, 09:00, 15:00, 21:00 UTC). The $p_{PV=2}$ parameter is used to determine the DT pressure at the top of the selected tropospheric vertical profile.

Tropospheric vertical profiles are selected according to several criteria:

1. Distance from the airport: Takeoffs and landings do not correspond stricto sensu to vertical profiles as aircraft travel some distance before reaching their cruise altitude. In order to limit the uncertainties induced by a potential horizontal heterogeneity, a maximum distance of 400 km from the airport is fixed for the vertical profile data selection. In practice, such a distance is sufficient for sampling the entire vertical profile in most flights, and remains reasonable considering the fact that the ozone vertical variability is expected to be higher than the horizontal one.

2. Potential vorticity: Based on PV vertical profiles, the 2 pvu value is used to locate the top of the tropospheric vertical profiles. This is illustrated in Fig. 1 with the Frankfurt–Boston flight of 19 March 2002 during which the DT altitude is estimated at 8.8 km. If the distance criteria is fullfilled before reaching DT, the $p_{PV=2}$ parameter is used to estimate the DT pressure (and thus to determine to which tropospheric sublayer points belong). However, PV values above 2 pvu may sometimes be encountered in the lower troposphere – due to recent deep stratospheric intrusions or convective processes – before decreasing again below the 2 pvu threshold until the tropopause. To avoid a misevaluation of the DT altitudes in such

ACPD
15, 23841–23891, 2015

cases, PV values are not considered point by point but over a window of several points – in our case, 60 points, which approximately corresponds to 1800 m on the vertical – and the tropopause is considered to be reached only when the minimum PV over that window exceeds 2 pvu (this value of 60 being empirically chosen to handle most of these situations) (or when the previous criteria is fulfilled).

Note that, as we are interested here in the real and not purely (with recent stratospheric contributions removed) tropospheric layer, stratospheric intrusions are not filtered in our methodology. Above the Frankfurt airport, a majority of vertical profiles (77 %) reach the tropopause while most of the remaining profiles (21 %) are selected according to the distance criteria. A similar proportion is found at Munich (74 and 24 %, respectively).

2.3 FLEXPART simulations

The FLEXPART Lagrangian particle dispersion model (Stohl et al., 2005) is used to investigate the origin of air masses sampled by aircraft in the different tropospheric sublayers above Frankfurt/Munich. Input meteorological data are taken from ECMWF operational analysis (00:00, 06:00, 12:00, 18:00 UTC) and forecasts (03:00, 09:00, 15:00, 21:00 UTC) and interpolated on a $1^\circ \times 1^\circ$ global longitude–latitude grid. The methodology used here basically consists in releasing along each vertical profile 1000 particles every 10 hPa and following them backward in time during 20 days, this duration corresponding approximately to the time during which a pollution plume is expected to remain significantly higher than the tropospheric background (Stohl et al., 2003a). Output are given on a $1^\circ \times 1^\circ$ global longitude–latitude grid, over 1 km width vertical layers up to 11 km plus a remaining layer ranging from 11 to 50 km (i.e. 12 vertical layers). Among the different FLEXPART outputs, this study will focus on the particles' residence time in the output grid cells. Note that, actually, the configuration is chosen so that to obtain residence times normalized by air density, thus expressed in $\mathrm{s\,m^3\,kg^{-1}}$ (which allows to couple FLEXPART outputs to emissions inventories in order to estimate regional contributions).

ACPD
15, 23841–23891, 2015

3 Climatology and trends of ozone and carbon monoxide results

Climatological vertical profiles of ozone and carbon monoxide around Frankfurt/Munich are described in Sect. 3.1. The variability of both compounds is analysed in Sect. 3.2, while annual and seasonal trends are investigated in Sect. 3.3.

3.1 Climatological vertical profiles

Annual and seasonal ozone and CO climatological vertical profiles are calculated over the whole period (1994–2012 for ozone, 2002–2012 for CO) and shown in Fig. 2. Average ozone mixing ratios in the tropospheric column range between 25–70 ppb, with a strong seasonal variability showing minimum values in winter (below 50 ppb) and maximum ones in spring/summer (up to 80 ppb). The ozone abundance clearly increases with altitude. Highest vertical gradients are found close to the surface all along the year (dry deposition and titration by NO) and at the vicinity of tropopause during spring and summer (exchanges with the stratospheric reservoir). The inflexion of vertical gradients at about 1 km a.g.l. has already been mentioned in Chevalier et al. (2007).

In free troposphere, vertical gradients are very low in winter and to a lesser extent in autumn, but significantly enhanced during spring and summer where concentrations quickly increase with altitude. The variability (expressed as the standard deviation normalized of the climatological profile) is about 15–30 % in free troposphere, with a minimum around 3 km whatever the season, but reaches much higher values in the first kilometer (30–80 %) and close to tropopause where it is likely driven by intense shallow and transient exchanges.

Carbon monoxide climatological vertical profiles show mixing ratios around 150 ppb at 1 km and 80 ppb high in altitude. As previously mentioned, mixing ratios in the first kilometer strongly increase as one moves closer to surface emissions, first and foremost emissions from the airport area (including aircraft emissions on runways) and potentially emissions from the neighbouring agglomeration. High seasonal variations are observed close to the surface, with concentrations in the first kilometer ranging

ACPD
15, 23841–23891, 2015

from 156 ppb in summer to 233 ppb in winter on average, the increase during that last season being notably due to a lower vertical mixing and higher emissions. However, contrary to ozone, carbon monoxide does not change significantly from one season to the other in free troposphere, seasonal climatological profiles always remaining at less than one sigma from the annual climatology (contrary to wintertime ozone above 4 km). Such moderate seasonal variations in altitude may be due to a higher contribution of secondary sources (biogenic hydrocarbon and methane oxidation) during summer that compensate the anthropogenic emissions decrease (Holloway et al., 2000).

3.2 Annual and monthly variability

Average monthly profiles are given in Fig. 3, and annual and monthly ozone and CO time series around Frankfurt/Munich in the three tropospheric sublayers are shown in Fig. 4.

3.2.1 Ozone variability.

As previously noted, mean tropospheric ozone increases with altitude, with average mixing ratios (over the whole period) of 44, 53 and 63 ppb in the LT, MT and UT, respectively. A clear seasonal pattern is emphasized in the lower troposphere, with a broad spring/summer maximum (including a secondary maximum in August) and a minimum in winter, in good accordance with seasonal variations observed at surface in Europe (Wilson et al., 2012). From the lower to the upper troposphere, a shift of the ozone maxima from May to July clearly appears in Fig. 3. Note that the ozone 5th percentile clearly peaks in April–May in the lower and mid-troposphere while the July maximum persists in the upper troposphere (see Fig. S4 and S5 in the Supplement). The 95th percentile shows a spring/summer maximum in all tropospheric layers. In average, the daily ozone variability at the monthly scale (represented by monthly standard deviations in Fig. 4) represents about 20 % of the mean in the lower and mid-troposphere, and 25 % in the upper troposphere. Highest monthly mixing ratios in the lower tropo-

ACPD
15, 23841–23891, 2015

sphere (above 60 ppb, the 99th percentile) are observed in August 1995, May 1998, August 2003, July 2006 (Fig. 4). The spring 1998 anomaly has been discussed by Koumoutsaris et al. (2008) and is related to the 1997 El Niño that have enhanced stratospheric–tropospheric exchanges (Ordóñez et al., 2007) and pollution export from Asia (higher convective activity and strengthening of the subtropical jet stream) and North America. Anomalies in summer 2003 and 2006 are related to the severe heat waves that struck a large part of Europe (Ordóñez et al., 2005; Solberg et al., 2008; Struzewska and Kaminski, 2008; see also Tressol et al. (2008) for a detailed analysis of the 2003 heat wave with MOZAIC measurements). Most of these ozone anomalies in the lower troposphere are not always distinguishable in the mid-troposphere, where highest concentrations (above 68 ppb, the 99th percentile) are encountered in summer 2002, 2004, 2006 and 2008. Similarly, highest monthly concentrations do not always coincide between the mid- and upper troposphere (see for instance the significant ozone mixing ratio observed in the UT during 2011 and 2012 summers). Nevertheless, on a yearly average, a very similar interannual variability is found between the three tropospheric sublayers as illustrated by high correlations (R = 0.87, 0.75 and 0.94 between the LT/MT, LT/UT and MT/UT, respectively).

3.2.2 Carbon monoxide variability

Carbon monoxide average mixing ratios of 143, 115 and 101 ppb are found in the LT, MT and UT, respectively. The CO enhancement in the European lower troposphere represents about half of the CO concentrations observed higher in altitude, which illustrates the high contribution of the CO background at the hemispheric scale. In comparison with ozone, the daily CO variability at the monthly scale is lower and similar in the three tropospheric sublayers (around 14–16 %). As shown in Fig. 3, the CO seasonal cycle is characterized by maximum mixing ratios in late winter/early spring in the whole troposphere. Minimum ones are encountered in summer/early autumn in the lower troposphere and are slightly shifted to late summer/early autumn higher in altitude. Such a seasonal pattern is rather consistent with maximum emissions and minimum photo-

ACPD
15, 23841–23891, 2015

chemical activity usually occuring around winter combined with a maximum secondary formation in summer. A rather similar seasonal pattern is observed with the CO 5th and 95th percentiles except that the peak is sharper (February–March) in the lower troposphere for the 95th percentile (see Fig. S4 and S5 in the Supplement).

3.3 Trends

Ozone trends are here investigated through linear regression calculations on 10-years moving periods in order to highlight dynamical changes in trends. Besides mean ozone concentrations, we also investigate trends on 5th and 95th percentiles that are taken as representative of baseline and peak ozone concentrations, respectively. Note that more detailed statistical approaches have been proposed for trend analysis, but as they are still widely used in the literature, linear regressions more easily allow comparisons with other published results. Ozone trends are reported in Table 1, and 10-years moving trends of mean ozone concentrations are shown in Fig. 5 (see Fig. S6 and S7 in the Supplement for the corresponding figures with 5th and 95th percentiles).

3.3.1 Ozone trends

Considering mean ozone concentrations over the whole 1994–2012 period, annual trends are positive in all layers and increase with altitude, but the statistical significance at a 95 % confidence level is almost reached only in the upper troposphere ($+0.22 \pm 0.23$ ppb yr^{-1}, against $+0.11 \pm 0.21$ and $+0.13 \pm 0.18$ ppb yr^{-1} in the LT and MT, respectively). In most tropospheric layers, these positive trends appear driven by increasing concentrations in winter ($+0.38 \pm 0.24$, $+0.31 \pm 0.24$ and $+0.36 \pm 0.31$ ppb yr^{-1} in the LT, MT and UT, respectively) and at a lesser extent in autumn. At lowest altitudes, such an increase in winter has already been observed at several sites in Europe and North America (Cooper et al., 2012; Derwent et al., 2013; Logan et al., 2012; Parrish et al., 2012; Wilson et al., 2012) and is mainly attributed to a reduced O_3 titration by NO due to decreasing NO_x emissions (e.g. Ordóñez et al.,

ACPD
15, 23841–23891, 2015

2005). Similar positive trends are found higher in altitude, which suggests that ozone is increasing at a large scale (if not hemispheric). Trend results on 10-years moving windows (Fig. 5) indicate that in the lower and mid-troposphere, the increase during these two seasons mainly occurs in the 1990s (visible in both background and high concentration episodes) before a stagnation in the 2000s. Interestingly, in the upper troposphere, the increase of wintertime concentrations mostly occurs in the 2000s (through increasing high concentrations) while no significant trend is found in autumn. Ozone trends do not appear related to altitude in winter and autumn, which is not the case for summer and spring that show increasing trends with altitude. For instance, albeit non significant (at a 95 % confidence interval), the mean ozone trend in summer moves from negative in the LT (-0.21 ± 0.34 ppb yr^{-1}) to near-zero in the MT (-0.01 ± 0.23 ppb yr^{-1}) and positive in the UT ($+0.21 \pm 0.31$ ppb yr^{-1}). The summertime decrease in the lower troposphere is associated to a decrease of high concentration episodes (-0.40 ± 0.51 ppb yr^{-1} for the ozone 95th percentile, thus significant at only one sigma) starting from the 2000s (in aggrement with Ordóñez et al., 2005, and Sicard et al., 2013), while the increase in the upper troposphere appears more linked to an increase of baseline ozone ($+0.30 \pm 0.30$ ppb yr^{-1} for the ozone 5th percentile). A slight increase of mean ozone trends with altitude is also displayed in spring, but the negative trend of 95th percentile in the lower troposphere is much reduced while the positive trend of 5th percentile spreads to the whole troposphere. Seasonal trend results thus strongly vary from one period to the other. During the last decade (2003–2012), the only significant trend is the decrease of summertime mean ozone (and annual ozone 95th percentile) in the LT.

Investigating ozone trends between 1995–2008 at various altitudes in troposphere above Frankfurt/Munich based on MOZAIC data, Logan et al. (2012) found statistically significant positive trends up to 8 km, with values around $+0.2$ ppb yr^{-1} up to 4 km and values between $+0.4$ and $+0.6$ ppb yr^{-1} between 4 and 8 km. Over the same period, our trends in the free and upper troposphere are also positive, but noticeably lower and statistically insignificant (around $+0.1 \pm 0.3$ ppb yr^{-1}) and without any major differ-

ACPD
15, 23841–23891, 2015

ence between tropospheric sublayers. Discrepancies may be due to the fact that Logan et al. (2012) applied a slightly different approach for calculating the trends (the annual cycle and the four seasonal trends being fit simultaneously considering monthly values). At about 3 km, Logan et al. (2012) highlighted a highly significant increase in winter and to a lesser extent in autumn, and insignificant trends in summer/autumn, in reasonable accordance with our results in the mid-troposphere except that again, our statistical significance is lower. Considering the 1998–2008 period, Logan et al. (2012) found no significant trends at any level and during any season, which remains consistent with our results during that period.

3.3.2 Carbon monoxide trends

As CO measurements in the MOZAIC-IAGOS program began only in December 2001, it does not appear relevant to investigate the trend evolution on moving periods as it was done with ozone. During the 2002–2012 period, CO significantly decreases in the whole troposphere, with trends of -2.62 ± 1.22, -1.87 ± 0.92 and -1.16 ± 0.88 ppb yr^{-1} in the lower, mid- and upper troposphere, respectively (as shown in Fig. 5). A negative trend in Europe was expected as decreasing CO mixing ratios have been already reported in many studies since the 1990s (e.g. Karlsdóttir et al., 2000; Novelli et al., 2003; Worden et al., 2013). This decrease of mean CO concentrations is actually associated to a decrease in occurrence of high CO episodes (for instance in the LT, the trend is -4.41 ± 1.34 ppb yr^{-1} for the 95th percentile compared to -1.91 ± 1.40 ppb yr^{-1} for the 5th percentile). Interestingly, trends highly depend on altitude, with decreasing negative values while one moves away from the surface. As European emissions are expected to contribute more to CO levels in the lower troposphere than in the mid- and upper troposphere compared to contributions from the other continents, this trend attenuation with altitude suggests that the decrease due to emission changes in Europe is higher than the decrease affecting the CO background advected toward that region. This may be due to changes in the long-range transport and/or a lower decrease of CO emissions in the rest of the world (or at least in the Northern Hemisphere). This latter

ACPD
15, 23841–23891, 2015

reason would be consistent with the emission trends given by MACC anthropogenic and GFAS biomass burning emission inventories that indicate between 2002 and 2012 a decrease of −41 % of CO emissions from both sources in Europe against only −1 % over the whole Northern Hemisphere (for details, see Table S1 in the Supplement). The higher emissions decrease of United States (−47 %) compensated by an increase of emissions in the rest of the Northern Hemisphere (in particular Asia) underlines the significant contribution of these other regions to CO levels in the European troposphere.

Albeit not always statistically significant, negative trends are found in troposphere during all seasons. The aforementioned decrease of the trend with altitude is observed whatever the season, except in winter. The difference is much more pronounced in summer (-3.06 ± 1.70 ppb yr^{-1} in the LT and trend 3.1 times lower in the UT) during which trends turn insignificant in the UT (similar strong differences are observed in autumn, with a factor of 2.7 between trends in the LT and UT, but trends all remains insignificant at a 95 % confidence level). During winter, trends are rather similar in the lower and mid-troposphere. Surprisingly, the wintertime trend in the LT is not statistically significant (-2.01 ± 2.33 ppb yr^{-1}). Observed mixing ratios show a high interannual variability, with maximum values (in 2003, 2006 and 2010) ranging between 166 and 180 ppb and minimum ones (in 2008, 2009 and 2012) remaining below 150 ppb. This interannual variability is mainly driven by the high CO episodes, as shown by the strong trend uncertainty of the 95th percentile (-1.15 ± 6.34 ppb yr^{-1} against -1.72 ± 1.92 ppb yr^{-1} for the 5th percentile). This may be partly due to a persistent influence of aircraft emissions – on tarmac and/or during the takeoff/landing phases (in case the MOZAIC-IAGOS aircraft closely follows other aircraft) – above 1 km, which may add some variability depending on the local dispersion conditions. But actually, the interannual variability found here in the LT with MOZAIC-IAGOS vertical profiles appears consistent with CO surface measurements obtained at four German stations from the WMO Global Atmosphere Watch (GAW) database (see Fig. S8 in the Supplement). Based on wintertime averages, the correlation with CO concentrations measured at the Ochsenkopf site (50.0° N, 11.8° W) is 0.64. It ranges between 0.75 and 0.85 at the

ACPD
15, 23841–23891, 2015

three other sites – Hohenpeissenberg (47.8° N, 11.0° W, 960 m; at 50 km south-west from Munich), Neuglobsow (53.1° N, 13.0° W), Schauinsland (47.9° N, 7.9° W) – which highlights the regional dimension of that interannual variability. The large variability of CO concentrations has already been noticed in other studies and may be linked to the variability of biomass burning emissions (Wotawa et al., 2001). Based on satellite measurements, a high positive anomaly on CO total columns in Europe and more generally in North Hemisphere has been reported by Worden et al. (2013) during most of the 2003 year, notably due to intense boreal fires. Conversely, the decline in 2008 may be due to lower global fire emissions (in particular in Equatorial Asia), potentially combined to the economic crisis effects (Worden et al., 2013).

4 Ozone seasonality changes

In the previous section, some differences in ozone trends have been highlighted depending on the season and the tropospheric sublayer. Here, we describe their impact on the ozone seasonal cycle above Frankfurt/Munich (Sect. 4.1), and compare results with observations from surface stations and ozone soundings (Sect. 4.2). In order to better understand differences obtained between tropospheric sublayers, results from the FLEXPART model are used to investigate the geographical origin of air masses sampled by MOZAIC-IAGOS aircraft (Sect. 4.3). In the light of this, ozone seasonal changes results are discussed in Sect. 4.4.

4.1 Evolution of the seasonal cycle at Frankfurt/Munich

The previous section has highlighted significant differences of trend depending on the season and the altitude above Frankfurt/Munich. This section now investigates how these different trends affect the ozone seasonal cycle in the troposphere. Assuming that this seasonal cycle follows a sinusoid, it can be fully characterized by three parameters: a baseline value defined here as the average over one or several years, an amplitude,

ACPD
15, 23841–23891, 2015

and a phase that determines at which period in the year the maximum of ozone is reached. Following Parrish et al. (2013), one can fit a sine function to the monthly time series over a period of several years:

$$\tilde{y}(t) = y_0 + \frac{a}{2}\sin\left(\frac{2\pi t}{12} + \varphi\right) \quad (1)$$

with t the time (in months), y_0 the baseline (in ppb), a the amplitude (in ppb) and φ the seasonal phase shift. Note that, using the properties of cosine and sinus functions, the fit can be easily performed by linear regression on $\cos(2\pi t/12)$ and $\sin(2\pi t/12)$. For clarity, one can consider φ_{month} defined as:

$$\varphi_{\text{month}} = \frac{365}{2\pi}\left(\frac{\pi}{2} - \varphi\right) \quad (2)$$

that now corresponds to the decimal month of maximum ozone (for instance, values of 1 and 6.5 correspond to an ozone peak the 1 January and the 15 June, respectively).

Results are presented in Fig. 6 considering windows of 10 years. The influence of that window width is discussed further below. First, it is worthwhile noting that errors – defined here as the root mean square of the quadratic sum of errors normalized by the number of points – related to sinusoidal fits (blue lines) do not vary significantly from one subperiod to the other, which allows a consistent analysis of the evolution of the various fit parameters.

4.1.1 Baseline

Over the whole period, the baseline slightly increases in all tropospheric sublayers (around 1–1.5 ppb, i.e. 2–3 %), despite a period of decrease between 1997–2006 and 2000–2009. The increase remains within the uncertainty range in the lower and mid-troposphere, in accordance with the small positive but not significant trends previously obtained by linear regression over the 1994–2012 period. These results confirm the tropospheric ozone leveling-off reported by many authors (Cooper et al., 2014; Cui et al., 2011; Oltmans et al., 2006).

ACPD
15, 23841–23891, 2015

4.1.2 Amplitude

Conversely, results show a decrease (around 1–2 ppb) of the amplitude of the ozone seasonal cycle in the three tropospheric sublayers along the 1995–2011 period. The negative trend is the most obvious in the lower troposphere where it continuously decreases from 19.1 ± 2.1 ppb in 1995–2004 to 15.8 ± 2.1 ppb in 2003–2012, this change being significant only at one sigma. The decrease is smaller in the mid- and upper troposphere and is statistically significant at one sigma only in the MT. Such a decrease of the seasonal amplitude is consistent with seasonal trends described in Sect. 3.3 where highest discrepancies between summer and winter trends are found in the lower troposphere (overall trends of -0.21 ± 0.34 and $+0.38 \pm 0.24$ ppb yr^{-1}, respectively).

4.1.3 Phase

Concerning the seasonal cycle phase, statistical significant differences are found between the different tropospheric sublayers with a peak occurring earlier in the LT compared to both the MT and UT. In 1995–2004, results indicate a maximum of the sinusoid in late spring in the lower troposphere (27 May) and early summer in the mid- and upper troposphere (6–7 June). It is worthwhile noting that it is rather consistent with averaged monthly profiles only in the LT, but not in the MT and UT where maximum O_3 concentrations are encountered in July, although June values are only slightly lower (−1.6 and −3.7 %, respectively). This is due to the fact that the ozone seasonal pattern does not follow exactly a sinusoide. This July maximum is driven by several high episodes during this month (with a high interannual variability). However, compared to the rest of the year, the weight of this July month is minor and thus it does not influence so much the fitted sinusoid that gives a maximum earlier in the year. In addition, this is not so problematic since we are here more interested in relative changes of the seasonal pattern than in the seasonal pattern itself.

In terms of trend along the 1995–2012 period, ozone peaks tend to occur earlier over the years. The tendency is more obvious in the lower troposphere and progres-

ACPD
15, 23841–23891, 2015

sively slips away higher in altitude. Based on these values of seasonal shift, linear trend results over the 1995–2012 period show that the highest and most statistically significant seasonal shift is observed in the LT with -10.6 ± 2.9 days decade^{-1} (at a 95 % confidence level, $p < 0.001$), more than two times higher than in the MT (-4.3 ± 2.4 days decade^{-1}, $p = 0.004$) and five times higher than in the UT (-2.0 ± 1.7 days decade^{-1}, $p = 0.03$). Note that the same analysis performed on 5th and 95th percentiles (not shown) rather than mean ozone concentrations shows a much stronger seasonal shift on the 5th percentile than on the 95th one, which means that the changes of phase mainly concern background concentrations. It is also worthwhile noting that consistent results are obtained, at least qualitatively, when the procedure is applied to the daily rather than monthly time series (not shown), the seasonal shifts being -13.4 ± 3.1, -5.2 ± 2.6 and -2.5 ± 2.1 days decade^{-1} for the LT, MT and UT, respectively.

4.2 Comparison with ozonesondes and surface observations

In this section, we apply the same procedure to ozone soundings (NDACC database) and surface measurements (GAW database) in Europe during the same 1995–2012 period. Only monitoring sites having observations all along the period are retained (12 surface sites and 3 ozonesonde sites; see Table 2 for informations on these sites).

4.2.1 Ground O_3 measurements

Most ground monitoring sites considered here are located in or close to Germany, which provides an overall picture of seasonal changes in that region. Shifts of the ozone seasonal pattern are shown in Fig. 7. Again, negative values indicate a shift toward earlier ozone maximum. For all sites except at Vindeln in Sweden, they are in the same direction than those obtained above Frankfurt/Munich, i.e. toward earlier ozone maximum. Values are highly variable from one site to the other, ranging between -14.0 and $+5.1$ days decade^{-1}, with different levels of statistical significance. The high-

ACPD
15, 23841–23891, 2015

est shifts are found in North-East Germany at Neuglobsow (-14.0 ± 2.6 days decade^{-1}) and Zingst (-11.0 ± 1.8), and the lowest ones at Westerland (-4.0 ± 2.3), Schauinsland (-2.6 ± 2.4) and Payerne (-5.3 ± 1.2). Explaining such discrepancies appears somewhat difficult. The extent of these shifts does not appear to be linked to levels of ozone concentration, as illustrated by the Kosetice site (Czech Republic) that shows all along the year twice as high O_3 concentrations compared to Waldhof (in the middle of Germany), but a very close seasonal shift (about 8–9 days decade^{-1}). Similarly, no clear relation between shifts and altitude arises from our results, as illustrated by the Sonnblick mountain site (Austria) that shows the same shift than the Kollumerwaard coastal site (the Netherlands). However, it is interesting to notice the decreasing shift with altitude between Rigi (1031 m a.s.l.) and Jungfraujoch (3580 m) sites that are distant by only 50 km. But considering the high spatial heterogeneity of seasonal shifts obtained here, it remains tricky to assert that this decrease with altitude corroborates our results obtained above Frankfurt/Munich.

In comparison, Parrish et al. (2013) have reported at four ground sites in Europe (two alpine sites including Jungfraujoch, the low elevation Hohenpeissenberg site and the Mace Head coastal site) shifts of the ozone seasonal cycle in the same direction (i.e. toward earlier O_3 maximum), but with lower rates than found here in the lower troposphere. At the three continental sites, rates of shift are statistically significant at the 95 % confidence limit and range between -5 and -7 days decade^{-1} since 1970s. At the Mace Head coastal site, the rate (-3 ± 3.7 days decade^{-1}) is lower and remains in the uncertainty range. Discrepancies are likely due to the fact that studied periods are different. As a faster phase change is found between 2005 and 2008 (their 3 last years) (see Fig. 2 in Parrish et al., 2013), restricting their analysis to our shorter period would likely lead to a higher seasonal shift (i.e. closer to our values).

ACPD
15, 23841–23891, 2015

4.2.2 Ozone soundings

Vertical profiles obtained by ozonesonde are more interesting for a comparison with our results above Frankfurt/Munich. We investigate seasonal changes at four tropospheric levels, delimited by the following pressures: 900, 800, 600, 400 and 300 hPa. Seasonal shifts between 1995–2004 and 2003–2012 are reported in Table 3. Seasonal shifts are statistically significant at Hohenpeissenberg but values do no monotonically decrease with altitude. Conversely, results at De Bilt show a high and significant (at a 95 % confidence level) shift in the lower troposphere that progressively decreases with altitude up to an insignificant shift in the 300–400 hPa layer. A rather similar behavior is found at Uccle, except that the shift goes in the opposite direction in the highermost level. It is to be noted that due to a much lower number of vertical profiles compared to MOZAIC-IAGOS (on average: 11, 4 and 12 ozonesondes per month at Hohenpeissenberg, De Bilt and Uccle, respectively), these results may be less reliable than at Frankfurt/Munich (Saunois et al., 2012).

4.3 Long-range transport and regional influences

Results obtained in the previous sections indicate that the ozone seasonal shift clearly depends on altitude. Therefore, in order to better characterize the geographical origin of air masses sampled by MOZAIC-IAGOS aircraft in the different tropospheric sublayers, we now investigate the density-normalized residence times (so-called residence times thereafter, for convenience) calculated with FLEXPART. We focus on residence times in the first kilometer above the surface (where air masses can potentially be loaded by local anthropogenic emissions) averaged over the 20 past days, but we will also discuss residence times at higher levels and over shorter time periods.

Footprints of 20 days average residence times between 0–1 km are presented in Fig. 8. These residence times are summed for different regions of the world, and Fig. 9 shows the monthly profile (averaged over the period 1994–2012) of their relative contribution.

ACPD
15, 23841–23891, 2015

4.3.1 Ocean vs. continents

In the Northern Hemisphere, air masses spend at surface approximately the same time above oceans and continents (not shown). The North Atlantic predominantly influences the lower troposphere above Frankfurt while the North Pacific contribution progressively increases at higher tropospheric levels. Interestingly, the oceanic influence on the mid- and upper troposphere is lower in summer compared to winter, and residence times at higher layers (than 0–1 km) do not show any compensation (the oceanic contribution being rather constant all along the year). It may thus induce a relatively lower dilution with clean marine air masses during summer, which should favor pollution transport toward Europe.

4.3.2 Europe and mid-Eurasia

In terms of residence times at surface, the influence of Europe is largely dominant in the lower troposphere (about 50 %). It is reduced by a factor of 3 in the mid-troposphere compared to the lower troposphere, but remains important regarding other regions. Conversely, the influence of Europe is minor in the upper troposphere (a factor of 10 lower than in the lower troposphere). Whatever the tropospheric sublayer, higher residence times in continental surface are found during summer. This is consistent with the fact that convective transport is the most efficient during that season (Auvray and Bey, 2005; Morel and Senesi, 2002), which likely explains this seasonal pattern, added to the fact that Germany is in Europe one of the major area of deep convection, often associated to thunderstorms (Duncan and Bey, 2004).

Residence times at the surface of mid-Eurasia contribute noticeably in the lower troposphere (about 10 %) and progressively decrease in the mid- and upper troposphere. As for Europe, such a decrease with altitude demonstrates that mid-Eurasia is here a local source region (i.e. air masses do not travel eastward all around the Northern Hemisphere), actually favoured by surface winds from south, south-east and east

ACPD
15, 23841–23891, 2015

sometimes induced by anticyclonic (cyclonic) conditions over Russia (Central Europe) (Aasa et al., 2004; Kozuchowski and Marciniak, 1988).

4.3.3 North and Central America

Boreal and temperate NA represent a major origin region for air masses sampled above Frankfurt, whatever the tropospheric sublayer. In the lower troposphere, boreal NA contributes about 20 % to the total residence time, compared to 5–10 % for temperate NA. The contribution of this last region is significantly enhanced in the mid-troposphere, where it is equivalent to boreal NA (about 20–30 %), and in the upper troposphere where it clearly dominates all the other regions of the world with a contribution around 30–40 %. Negligeable in the lower troposphere, the contribution of Central America progressively increases at higher altitudes, up to about 10 % in the upper troposphere. Comparing results in the mid- and upper troposphere, it is interesting to notice the southward shift as one moves toward higher altitudes, with a decreasing contribution of boreal NA and an increasing contribution of temperate NA and Central America. In contrast to these two last regions, (absolute) residence times at the surface of boreal NA are higher in air masses sampled in the lower troposphere than in the upper troposphere.

A wide literature has been published on transatlantic transport. Through a fast uplifting of boundary layer air masses up to the mid- and upper troposphere where strong westerlies efficiently advect air masses toward downwind regions, warm conveyor belts (WCB) ahead of cold fronts are known to be one of the major pollution export pathway from NA to Europe (Cooper et al., 2002, 2004; Liang et al., 2004; Stohl and Trickl, 1999). This pathway is particularly important along the NA south-eastern coast where most WCB start (Stohl, 2001) and is maximum during winter when WCB are the strongest and the most frequent – about one order of magnitude more frequent than in summer according to the 15-years climatology of Eckhardt et al. (2004) – and jet stream wind speeds the highest – around a factor of 2 higher than in summer according to ERA-40 reanalysis between 1979 and 2001 (Archer and Caldeira, 2008).

ACPD
15, 23841–23891, 2015

Running northwesterly behind cold fronts, post cold fronts (PCF) represent another important airstream characterized by a lack of precipitation and sunny conditions that can favor photochemical production and low-level transport of accumulated pollution that can be subsequently lifted at higher tropospheric levels by next cold fronts. In addition, during winter, depending on the position and strength of the Azores High and Icelandic Low, air masses coming from US tend to be quickly zonally advected toward Europe while in late spring and early summer, due to the Azores anticyclone strengthening and the Icelandic Low weakening, air masses coming from US are sent back toward west through an anticyclonic circulation, this phenomena being particularly important in lowest tropospheric levels (Auvray and Bey, 2005). These mechanisms likely explain the seasonality of residence times over Central America that show higher values during winter/spring and lower ones during summer, although with a substancial variability from one month to the other. However, no clear seasonal pattern is found for boreal NA (except maybe lower springtime values obtained in the upper troposphere). Concerning temperate NA, residence times tend to be slightly higher (lower) during winter (summer), but seasonal variations vanish in the mid-troposphere and show a very clear summer maxima in the upper troposphere. Investigating the influence of the North Atlantic Oscillation on residence times would likely provide valuable informations but is beyond the scope of this study.

It is worthwhile noting that high residence times can reflect a larger number of particles trajectories travelling in the cell and/or a longer time spent within that cell. Cluster trajectories indicate that a higher proportion of particle trajectories have travelled at the surface of temperate NA in winter in comparison to summer.

4.3.4 Asia

In the lower troposphere, results indicate moderate residence times above Asia (about 5–10 %), essentially in boreal Asia. Higher in altitude, in both relative and absolute terms, the influence of this last region remains rather unchanged, in contrast with Central Asia and to a lesser extent South-East Asia that show increasing residence times,

ACPD
15, 23841–23891, 2015

up to 20 and 5–10 %, respectively in the upper troposphere. The clearest seasonal pattern is given by South-East Asia that shows highest values in winter/early spring and lowest ones in summer. A similar seasonality is found in the lower troposphere for boreal and Central Asia. However, for these two regions, the seasonal pattern is less clear in the mid- and upper troposphere, where results show some still high residence times in summer.

During summer, a major role is played by the East Asia Summer Monsoon (EASM) that is characterized by intense deep convection mechanisms that favor the upward transport in the upper troposphere. At these altitudes, the easterly flow induced by the Tibetan anticyclone dominates and efficiently carries polluted air masses eastward, toward Middle East, while at lower altitudes in the mid-troposphere, the Tibetan anticyclone has a lower intensity and the flow is governed by weak westerlies (Liu et al., 2003; Park et al., 2009; Ricaud et al., 2014). At surface, the Pacific High also plays an important role through the associated southeasterly winds that bring clean marine air masses toward the continent (Stohl, 2004). This likely explains the minimum residence times over South-East Asia obtained during that season. Northward from the monsoon area, both deep convection and transport associated to frontal systems participate to pollution exports (Liang et al., 2004), which likely explains the still high residence times over Central and boreal Asia in summer (in contrast to South-East Asia). In autumn, a cold high-pressure system known as the Siberia-Mongolia High (SMH) starts to develop and extend over the continent (Chang et al., 2006). It reaches its maximum in winter, leading to prevailing anticyclonic conditions over China that trap pollution in the boundary layer, confining northwesterly continental outflows close to the surface (Stohl, 2004). The east coast of Asia is a favoured region for cyclogenesis and WCB can then transport air masses across the Pacific, which may explain the still high residence times over Central Asia obtained during that season. Strong northeasterly winds blow at surface in the South China Sea (Chang et al., 2005), which may send back air masses toward South-East Asia. The higher wintertime jet streams likely considerably help continental outflows reach remote regions as Europe (Archer and Caldeira, 2008). During

ACPD
15, 23841–23891, 2015

spring, WCB represent the major pathway for Asian pollution export toward western North Pacific and downwind regions (Liang et al., 2004). Note also that in contrast with North Pacific (and North Atlantic) where WCB fluxes are maximum in winter, Eckhardt et al. (2004) showed some evidence of WCB fluxes over Asia peaking in spring.

With the STOCHEM global 3D Lagrangian chemistry-transport model, Derwent et al. (2004) discussed the regional contributions of surface ozone at several sites in Europe, as well as the contribution of stratosphere–troposphere exchanges (STE). At the Waldhof site (at about 50 km from Frankfurt), they found annual contributions of 47, 22 and 12 % from European, North America and Asia emissions, respectively (the remaining 20 % being related to STE). As the two approaches are different, our results are not directly comparable to those of Derwent et al. (2004) but appear qualitatively consistent with them.

4.4 Discussion

This study confirms that the ozone seasonal pattern in Central/Western Europe is changing, at least since the mid-1990s, moving toward lower amplitude and earlier ozone maxima. Thanks to vertical profile observations, it brings an interesting contribution by highlighting that these seasonal changes above Frankfurt/Munich clearly depend on altitude, with the highest shift in the lower troposphere and much lower ones in the mid- and upper troposphere. It is worthwhile noting that MOZAIC-IAGOS observations above Frankfurt/Munich likely represent the densest dataset of ozone vertical profiles in the world, which gives robustness to our results. Qualitatively, a similar behavior is observed in ozonesonde observations at two sites among three, but the reliability of these results is limited by a much lower number of vertical profiles. However, a high variability from one site to the other in Europe affects both the rate of decrease with altitude and the shift extent itself, as confirmed by results obtained at ground stations.

The trend analysis (Sect. 3.3) shows that in the lower troposphere, the ozone seasonal cycle is changing toward earlier maxima mainly due to the combined effect of

ACPD
15, 23841–23891, 2015

(i) a progressive shift from positive to near-zero trends in spring and (ii) a shift from positive to strongly negative trends in summer (associated to a progressive reduction of high concentration episodes); i.e. a relatively higher decrease in summer compared to spring. While a rather similar behavior is observed higher in the troposphere during spring, the main difference concerns summertime during which no significant negative trend is found in high concentration episodes. Note however that over the whole period, the (positive) trend in spring is higher than in summer in all tropospheric sublayers, but discrepancies between both seasons decrease with altitude, which means that the ozone seasonal cycle is also changing in the same direction in highest tropospheric levels but at a much lower rate.

Parrish et al. (2013) exhaustively discussed several reasons that may explain this changing phase at surface in Europe, including changes in downward transport of stratospheric O_3, long-range transport, O_3 precursor's emissions and their spatial distribution, photochemical production and the potential influence of climate change. Our study does not provide an unambiguous explanation to either the seasonal trends discrepancies or the subsequent seasonal shifts (which would ideally require the use of global models able to correctly restitute both ozone seasonal patterns and trends throughout the troposphere). In the lower troposphere, the decrease of high ozone summertime episodes is likely mainly due to the precursor emissions control in Europe (the main origin region of air masses sampled by aircraft, see Sect. 4.3). A similar situation is observed at many surface sites in North America (the second major origin region) where emissions are also decreasing (Cooper et al., 2012; Hogrefe et al., 2011), but it is not clear how high is the impact of such summertime changes on the European lower troposphere as Auvray and Bey (2005) showed a North America ozone contribution in Europe peaking in spring at the surface (and summer in free troposphere) according to the GEOS-Chem model. Higher in the troposphere, our long-range transport analysis demonstrates an increasing influence of air masses coming from North America and Asia. In contrast with the surface, the ozone contributions from Europe, North America and Asia in free troposphere (more or less sharply) peak in summer

ACPD
15, 23841–23891, 2015

(Auvray and Bey, 2005). While Europe and North America contributions are expected to decrease, the Asia one is likely increasing due to the lack of emission control. The Asian pollution outflow (direct pollution export and/or photochemical production during transport) may thus compensate in highest tropospheric levels the expected decrease of summertime ozone, in particular in the upper troposphere where the influence of Asia (in terms of air masses residence time) is the strongest. This would be consistent with the negative CO (positive O_3) annual trend that is maximum (minimum) in the lower troposphere and progressively decreases (increases) as one moves toward higher altitudes (although most O_3 trends are not significant at a 95 % confidence level). In addition, for both O_3 and CO, trend differences between the lower and upper troposphere are maximum in summer and minimum in winter. However, if the Asian contribution to ozone is increasing in the upper troposphere, leading to enhanced ozone concentrations in summer, our study does not allow to assess its importance relatively to other sources like summertime biomass burning events, in particular over boreal North America where air masses spend a large time, notably during warm months. In particular, uncertainties persist on the ozone production in wildfire plumes along transport (Real et al., 2007).

In terms of stratospheric contributions, stratosphere-to-troposphere ozone fluxes are known to peak in spring (Auvray and Bey, 2005; James et al., 2003; Tang et al., 2011) due to both enhanced downward transport and maximum concentrations in lowermost stratosphere (e.g. Thouret et al., 2006). Some changes of these fluxes in spring relatively to summer may thus also play a role in the seasonal discrepancies observed here, although to our knowledge no previous studies have highlighted such evolution of the seasonal pattern of stratosphere-to-troposphere transport.

5 Summary and conclusions

An extensive database of ozone and CO vertical profiles above worldwide airports is available from the MOZAIC-IAGOS program since 1994 and 2002, respectively. In this

ACPD
15, 23841–23891, 2015

study, we investigate the climatology, variability and trends of ozone and CO observations obtained above the Frankfurt and Munich airports whose combination represents the densest and longest MOZAIC-IAGOS dataset. We focus on troposphere, each vertical profile being subdivided in three tropospheric sublayers – the lower, mid- and upper troposphere (LT, MT and UT, respectively) – based on the potential vorticity extracted from ECMWF meteorological data. Main results are given below (all trends are given with uncertainties at a 95 % confidence level):

1. Seasonal variations: Ozone monthly mean profiles in all tropospheric sublayers show a minimum in December while the maxima vary from May in the lower troposphere to July in the mid- and upper troposphere. Carbon monoxide monthly mean profiles peak in March/April in the whole troposphere, and reach a broad minima in July–October in the lower troposphere, refined to September/October in the mid- and upper troposphere.

2. Annual and seasonal ozone trends: On an annual basis over the 1994–2012 period, tropospheric ozone shows increasing upward trends with altitude, from $+0.11 \pm 0.21$ and $+0.13 \pm 0.18$ ppb yr^{-1} in the lower and mid-troposphere to $+0.22 \pm 0.23$ ppb yr^{-1} in the upper troposphere (significant at only one sigma), these positive trends being mainly driven by an increase of ozone concentrations in the 1990s. On a seasonal basis, highest ozone upward trends are found in winter (around $+0.38 \pm 0.24$ ppb yr^{-1}). Seasonal trend results also indicate that discrepancies between the lower and upper troposphere are mainly due to the summertime trend (that goes from -0.21 ± 0.34 to $+0.21 \pm 0.31$ ppb yr^{-1}, respectively) and at a lesser extent the spring trend ($+0.14 \pm 0.25$ and $+0.26 \pm 0.30$ ppb yr^{-1}, respectively). The summertime decrease in the lower troposphere appears mainly driven by a reduction of high ozone episodes.

3. Annual and seasonal CO trends: Over the 2002–2012 period, carbon monoxide is decreasing whatever the tropospheric sublayer and the season. As for ozone, trends decrease with altitude, from -2.62 ± 1.22 ppb yr^{-1} in the lower troposphere

ACPD
15, 23841–23891, 2015

to -1.16 ± 0.88 ppb yr^{-1} in the upper troposphere, with major differences in summer (-3.06 ± 1.70 and -0.99 ± 1.21 ppb yr^{-1}, respectively).

This study also investigates the changes in the ozone seasonal cycle (by fitting sinusoides over 10-years moving windows) with a focus on the phase. Results highlight a statistically significant change of the phase in the lower troposphere, ozone maxima occurring earlier by -10.6 ± 2.9 days decade^{-1} on average (at a 95 % confidence level), in general agreement with previous results from the literature (Parrish et al., 2013). Observations at most surface stations in Central Europe show seasonal shifts in the same direction (toward earlier maxima), but with a strong variability from one station to the other. A major contribution of this study concerns the dependence on altitude of this seasonal shift, as it is found to decrease by a factor of two in the mid-troposphere (-4.3 ± 2.4 days decade^{-1}) and five in the upper troposphere (-2.0 ± 1.7 days decade^{-1}). Qualitatively, a similar dependence on altitude is obtained with ozonesonde observations at two among three sites in Europe.

The FLEXPART Lagrangian particle dispersion model is used to investigate the geographical origin of air masses sampled at the different tropospheric sublayers. Results show a high influence of Europe in the lower troposphere that noticeably decreases as one moves toward higher tropospheric levels for the benefit of North America and Asia. Some strong seasonal variations are also highighted for most regions. Combined with the seasonal trend and phase changes results, it suggests that the Asian contribution to ozone in the upper troposphere may compensate during summer the decrease associated to the emission control in place in Europe and North America. Further studies are obviously required to quantitatively assess such a scenario.

The Supplement related to this article is available online at doi:10.5194/acpd-15-23841-2015-supplement.

ACPD
15, 23841–23891, 2015

References

Aasa, A., Jaagus, J., Ahas, R., and Sepp, M.: The influence of atmospheric circulation on plant phenological phases in central and eastern Europe, Int. J. Climatol., 24, 1551–1564, doi:10.1002/joc.1066, 2004.

Archer, C. L. and Caldeira, K.: Historical trends in the jet streams, Geophys. Res. Lett., 35, L08803, doi:10.1029/2008GL033614, 2008.

Ashmore, M. R.: Assessing the future global impacts of ozone on vegetation, Plant Cell Environ., 28, 949–964, doi:10.1111/j.1365-3040.2005.01341.x, 2005.

Auvray, M. and Bey, I.: Long-range transport to Europe: seasonal variations and implications for the European ozone budget, J. Geophys. Res., 110, D11303, doi:10.1029/2004JD005503, 2005.

Bethan, S., Vaughan, G., and Reid, S. J.: A comparison of ozone and thermal tropopause heights and the impact of tropopause definition on quantifying the ozone content of the troposphere, Q. J. Roy. Meteor. Soc., 122, 929–944, doi:10.1002/qj.49712253207, 1996.

Chang, C.-P., Harr, P. A., and Chen, H.-J.: Synoptic disturbances over the equatorial South China Sea and western maritime continent during boreal winter, Mon. Weather Rev., 133, 489–503, doi:10.1175/MWR-2868.1, 2005.

Chang, C.-P., Wang, Z., and Hendon, H.: The Asian winter monsoon, in: The Asian Monsoon, Springer Praxis Books, Chichester, UK, 89–127, 2006.

Chevalier, A., Gheusi, F., Delmas, R., Ordóñez, C., Sarrat, C., Zbinden, R., Thouret, V., Athier, G., and Cousin, J.-M.: Influence of altitude on ozone levels and variability in the lower troposphere: a ground-based study for western Europe over the period 2001–2004, Atmos. Chem. Phys., 7, 4311–4326, doi:10.5194/acp-7-4311-2007, 2007.

Cooper, O. R., Moody, J. L., Parrish, D. D., Trainer, M., Ryerson, T. B., Holloway, J. S., Hübler, G., Fehsenfeld, F. C., and Evans, M. J.: Trace gas composition of midlatitude cyclones over the western North Atlantic Ocean: A conceptual model, J. Geophys. Res., 107, 4056, doi:10.1029/2001JD000901, 2002.

Cooper, O. R., Forster, C., Parrish, D., Trainer, M., Dunlea, E., Ryerson, T., Hübler, G., Fehsenfeld, F., Nicks, D., Holloway, J., de Gouw, J., Warneke, C., Roberts, J. M., Flocke, F., and Moody, J.: A case study of transpacific warm conveyor belt transport: influence of merging airstreams on trace gas import to North America, J. Geophys. Res.-Atmos., 109, D23S08, doi:10.1029/2003JD003624, 2004.

ACPD
15, 23841–23891, 2015

Cooper, O. R., Gao, R.-S., Tarasick, D., Leblanc, T., and Sweeney, C.: Long-term ozone trends at rural ozone monitoring sites across the United States, 1990–2010, J. Geophys. Res.-Atmos., 117, D22307, doi:10.1029/2012JD018261, 2012.

Cooper, O. R., Parrish, D. D., Ziemke, J., Balashov, N. V., Cupeiro, M., Galbally, I. E., Gilge, S., Horowitz, L., Jensen, N. R., Lamarque, J.-F., Naik, V., Oltmans, S. J., Schwab, J., Shindell, D. T., Thompson, A. M., Thouret, V., Wang, Y., and Zbinden, R. M.: Global distribution and trends of tropospheric ozone: An observation-based review, Elem. Sci. Anthr., 2, 000029, doi:10.12952/journal.elementa.000029, 2014.

Cui, J., Pandey Deolal, S., Sprenger, M., Henne, S., Staehelin, J., Steinbacher, M., and Nédélec, P.: Free tropospheric ozone changes over Europe as observed at Jungfraujoch (1990–2008): an analysis based on backward trajectories, J. Geophys. Res., 116, D10304, doi:10.1029/2010JD015154, 2011.

Derwent, R. G., Stevenson, D. S., Collins, W. J., and Johnson, C. E.: Intercontinental transport and the origins of the ozone observed at surface sites in Europe, Atmos. Environ., 38, 1891–1901, doi:10.1016/j.atmosenv.2004.01.008, 2004.

Derwent, R. G., Simmonds, P. G., Manning, A. J., and Spain, T. G.: Trends over a 20 year period from 1987 to 2007 in surface ozone at the Atmospheric Research station, Mace Head, Ireland, Atmos. Environ., 41, 9091–9098, doi:10.1016/j.atmosenv.2007.08.008, 2007.

Derwent, R. G., Manning, A. J., Simmonds, P. G., Spain, T. G., and O'Doherty, S.: Analysis and interpretation of 25 years of ozone observations at the Mace Head Atmospheric Research Station on the Atlantic Ocean coast of Ireland from 1987 to 2012, Atmos. Environ., 80, 361–368, doi:10.1016/j.atmosenv.2013.08.003, 2013.

Duncan, B. N. and Bey, I.: A modeling study of the export pathways of pollution from Europe: seasonal and interannual variations (1987–1997), J. Geophys. Res., 109, D08301, doi:10.1029/2003JD004079, 2004.

Eckhardt, S., Stohl, A., Wernli, H., James, P., Forster, C., and Spichtinger, N.: A 15 year climatology of warm conveyor belts, J. Climate, 17, 218–237, 2004.

Hogrefe, C., Hao, W., Zalewsky, E. E., Ku, J.-Y., Lynn, B., Rosenzweig, C., Schultz, M. G., Rast, S., Newchurch, M. J., Wang, L., Kinney, P. L., and Sistla, G.: An analysis of long-term regional-scale ozone simulations over the Northeastern United States: variability and trends, Atmos. Chem. Phys., 11, 567–582, doi:10.5194/acp-11-567-2011, 2011.

Holloway, T., Levy, H., and Kasibhatla, P.: Global distribution of carbon monoxide, J. Geophys. Res., 105, 12123, doi:10.1029/1999JD901173, 2000.

ACPD
15, 23841–23891, 2015

Holton, J. R., Haynes, P. H., McIntyre, M. E., Douglass, A. R., Rood, R. B., and Pfister, L.: Stratosphere–troposphere exchange, Rev. Geophys., 33, 403–439, doi:10.1029/95RG02097, 1995.

IPCC: Climate Change 2013: The Physical Science Basis, available at: http://www.ipcc.ch/report/ar5/wg1/ (last access: 31 August 2015), 2013.

James, P., Stohl, A., Forster, C., Eckhardt, S., Seibert, P., and Frank, A.: A 15 year climatology of stratosphere–troposphere exchange with a Lagrangian particle dispersion model: 1. methodology and validation, J. Geophys. Res., 108, 8519, doi:10.1029/2002JD002637, 2003.

Jerrett, M., Burnett, R. T., Pope, C. A., Ito, K., Thurston, G., Krewski, D., Shi, Y., Calle, E., and Thun, M.: Long-term ozone exposure and mortality., New Engl. J. Med., 360, 1085–1095, doi:10.1056/NEJMoa0803894, 2009.

Karlsdóttir, S., Isaksen, I. S. A., Myhre, G., and Berntsen, T. K.: Trend analysis of O_3 and CO in the period 1980–1996: a three-dimensional model study, J. Geophys. Res., 105, 28907, doi:10.1029/2000JD900374, 2000.

Koumoutsaris, S., Bey, I., Generoso, S., and Thouret, V.: Influence of El Niño-Southern Oscillation on the interannual variability of tropospheric ozone in the northern midlatitudes, J. Geophys. Res., 113, D19301, doi:10.1029/2007JD009753, 2008.

Kozuchowski, K. and Marciniak, K.: Variability of mean monthly temperatures and semi-annual precipitation totals in Europe in relation to hemispheric circulation patterns, J. Climatol., 8, 191–199, doi:10.1002/joc.3370080206, 1988.

Liang, Q., Jaeglé, L., Jaffe, D. A., Weiss-Penzias, P., Heckman, A., and Snow, J. A.: Long-range transport of Asian pollution to the Northeast Pacific: seasonal variations and transport pathways of carbon monoxide, J. Geophys. Res.-Atmos., 109, D23S07, doi:10.1029/2003JD004402, 2004.

Liu, H., Jacob, D. J., Bey, I., Yantosca, R. M., Duncan, B. N., and Sachse, G. W.: Transport pathways for Asian pollution outflow over the Pacific: interannual and seasonal variations, J. Geophys. Res., 108, 8786, doi:10.1029/2002JD003102, 2003.

Logan, J. A., Megretskaia, I. A., Miller, A. J., Tiao, G. C., Choi, D., Zhang, L., Stolarski, R. S., Labow, G. J., Hollandsworth, S. M., Bodeker, G. E., Claude, H., De Muer, D., Kerr, J. B., Tarasick, D. W., Oltmans, S. J., Johnson, B., Schmidlin, F., Staehelin, J., Viatte, P., and Uchino, O.: Trends in the vertical distribution of ozone: a comparison of two analyses of ozonesonde data, J. Geophys. Res., 104, 26373, doi:10.1029/1999JD900300, 1999.

ACPD
15, 23841–23891, 2015

Logan, J. A., Staehelin, J., Megretskaia, I. A., Cammas, J.-P., Thouret, V., Claude, H., De Backer, H., Steinbacher, M., Scheel, H.-E., Stübi, R., Fröhlich, M., and Derwent, R.: Changes in ozone over Europe: analysis of ozone measurements from sondes, regular aircraft (MOZAIC) and alpine surface sites, J. Geophys. Res., 117, D09301, doi:10.1029/2011JD016952, 2012.

Moise, T. and Rudich, Y.: Reactive uptake of ozone by proxies for organic aerosols: surface vs. bulk processes, J. Geophys. Res., 105, 14667, doi:10.1029/2000JD900071, 2000.

Moise, T. and Rudich, Y.: Reactive uptake of ozone by aerosol-associated unsaturated fatty acids: kinetics, mechanism, and products, J. Phys. Chem. A, 106, 6469–6476, doi:10.1021/jp025597e, 2002.

Morel, C. and Senesi, S.: A climatology of mesoscale convective systems over Europe using satellite infrared imagery. I: Methodology, Q. J. Roy. Meteor. Soc., 128, 1953–1971, doi:10.1256/003590002320603485, 2002.

Nedelec, P., Cammas, J.-P., Thouret, V., Athier, G., Cousin, J.-M., Legrand, C., Abonnel, C., Lecoeur, F., Cayez, G., and Marizy, C.: An improved infrared carbon monoxide analyser for routine measurements aboard commercial Airbus aircraft: technical validation and first scientific results of the MOZAIC III programme, Atmos. Chem. Phys., 3, 1551–1564, doi:10.5194/acp-3-1551-2003, 2003.

Novelli, P. C., Masarie, K. A., Lang, P. M., Hall, B. D., Myers, R. C., and Elkins, J. W.: Reanalysis of tropospheric CO trends: effects of the 1997–1998 wildfires, J. Geophys. Res., 108, 4464, doi:10.1029/2002JD003031, 2003.

Oltmans, S. J., Lefohn, A. S., Scheel, H. E., Harris, J. M., Levy, H., Galbally, I. E., Brunke, E.-G., Meyer, C. P., Lathrop, J. A., Johnson, B. J., Shadwick, D. S., Cuevas, E., Schmidlin, F. J., Tarasick, D. W., Claude, H., Kerr, J. B., Uchino, O., and Mohnen, V.: Trends of ozone in the troposphere, Geophys. Res. Lett., 25, 139–142, doi:10.1029/97GL03505, 1998.

Oltmans, S. J., Lefohn, A. S., Harris, J. M., Galbally, I., Scheel, H. E., Bodeker, G., Brunke, E., Claude, H., Tarasick, D., Johnson, B. J., Simmonds, P., Shadwick, D., Anlauf, K., Hayden, K., Schmidlin, F., Fujimoto, T., Akagi, K., Meyer, C., Nichol, S., Davies, J., Redondas, A., and Cuevas, E.: Long-term changes in tropospheric ozone, Atmos. Environ., 40, 3156–3173, doi:10.1016/j.atmosenv.2006.01.029, 2006.

Oltmans, S. J., Lefohn, A. S., Shadwick, D., Harris, J. M., Scheel, H. E., Galbally, I., Tarasick, D. W., Johnson, B. J., Brunke, E.-G., Claude, H., Zeng, G., Nichol, S., Schmidlin, F., Davies, J., Cuevas, E., Redondas, A., Naoe, H., Nakano, T., and Kawasato, T.: Recent tro-

ACPD
15, 23841–23891, 2015

pospheric ozone changes – a pattern dominated by slow or no growth, Atmos. Environ., 67, 331–351, doi:10.1016/j.atmosenv.2012.10.057, 2013.
Ordóñez, C., Mathis, H., Furger, M., Henne, S., Hüglin, C., Staehelin, J., and Prévôt, A. S. H.: Changes of daily surface ozone maxima in Switzerland in all seasons from 1992 to 2002 and discussion of summer 2003, Atmos. Chem. Phys., 5, 1187–1203, doi:10.5194/acp-5-1187-2005, 2005.
Ordóñez, C., Brunner, D., Staehelin, J., Hadjinicolaou, P., Pyle, J. A., Jonas, M., Wernli, H., and Prévôt, A. S. H.: Strong influence of lowermost stratospheric ozone on lower tropospheric background ozone changes over Europe, Geophys. Res. Lett., 34, L07805, doi:10.1029/2006GL029113, 2007.
Paoletti, E.: Impact of ozone on Mediterranean forests: a review, Environ. Pollut., 144, 463–474, doi:10.1016/j.envpol.2005.12.051, 2006.
Park, M., Randel, W. J., Emmons, L. K., and Livesey, N. J.: Transport pathways of carbon monoxide in the Asian summer monsoon diagnosed from Model of Ozone and Related Tracers (MOZART), J. Geophys. Res., 114, D08303, doi:10.1029/2008JD010621, 2009.
Parrish, D. D., Law, K. S., Staehelin, J., Derwent, R., Cooper, O. R., Tanimoto, H., Volz-Thomas, A., Gilge, S., Scheel, H.-E., Steinbacher, M., and Chan, E.: Long-term changes in lower tropospheric baseline ozone concentrations at northern mid-latitudes, Atmos. Chem. Phys., 12, 11485–11504, doi:10.5194/acp-12-11485-2012, 2012.
Parrish, D. D., Law, K. S., Staehelin, J., Derwent, R., Cooper, O. R., Tanimoto, H., Volz-Thomas, A., Gilge, S., Scheel, H.-E., Steinbacher, M., and Chan, E.: Lower tropospheric ozone at northern midlatitudes: changing seasonal cycle, Geophys. Res. Lett., 40, 1631–1636, doi:10.1002/grl.50303, 2013.
Real, E., Law, K. S., Weinzierl, B., Fiebig, M., Petzold, A., Wild, O., Methven, J., Arnold, S., Stohl, A., Huntrieser, H., Roiger, A., Schlager, H., Stewart, D., Avery, M., Sachse, G., Browell, E., Ferrare, R., and Blake, D.: Processes influencing ozone levels in Alaskan forest fire plumes during long-range transport over the North Atlantic, J. Geophys. Res., 112, D10S41, doi:10.1029/2006JD007576, 2007.
Ricaud, P., Sič, B., El Amraoui, L., Attié, J.-L., Zbinden, R., Huszar, P., Szopa, S., Parmentier, J., Jaidan, N., Michou, M., Abida, R., Carminati, F., Hauglustaine, D., August, T., Warner, J., Imasu, R., Saitoh, N., and Peuch, V.-H.: Impact of the Asian monsoon anticyclone on the variability of mid-to-upper tropospheric methane above the Mediterranean Basin, Atmos. Chem. Phys., 14, 11427–11446, doi:10.5194/acp-14-11427-2014, 2014.

ACPD
15, 23841–23891, 2015

Saunois, M., Emmons, L., Lamarque, J.-F., Tilmes, S., Wespes, C., Thouret, V., and Schultz, M.: Impact of sampling frequency in the analysis of tropospheric ozone observations, Atmos. Chem. Phys., 12, 6757–6773, doi:10.5194/acp-12-6757-2012, 2012.

Sicard, P., De Marco, A., Troussier, F., Renou, C., Vas, N., and Paoletti, E.: Decrease in surface ozone concentrations at Mediterranean remote sites and increase in the cities, Atmos. Environ., 79, 705–715, doi:10.1016/j.atmosenv.2013.07.042, 2013.

Simmonds, P. G., Derwent, R. G., Manning, A. L., and Spain, G.: Significant growth in surface ozone at Mace Head, Ireland, 1987–2003, Atmos. Environ., 38, 4769–4778, doi:10.1016/j.atmosenv.2004.04.036, 2004.

Solberg, S., Hov, Ø., Søvde, A., Isaksen, I. S. A., Coddeville, P., De Backer, H., Forster, C., Orsolini, Y., and Uhse, K.: European surface ozone in the extreme summer 2003, J. Geophys. Res., 113, D07307, doi:10.1029/2007JD009098, 2008.

Stevenson, D. S., Dentener, F. J., Schultz, M. G., Ellingsen, K., van Noije, T. P. C., Wild, O., Zeng, G., Amann, M., Atherton, C. S., Bell, N., Bergmann, D. J., Bey, I., Butler, T., Cofala, J., Collins, W. J., Derwent, R. G., Doherty, R. M., Drevet, J., Eskes, H. J., Fiore, A. M., Gauss, M., Hauglustaine, D. A., Horowitz, L. W., Isaksen, I. S. A., Krol, M. C., Lamarque, J.-F., Lawrence, M. G., Montanaro, V., Müller, J.-F., Pitari, G., Prather, M. J., Pyle, J. A., Rast, S., Rodriguez, J. M., Sanderson, M. G., Savage, N. H., Shindell, D. T., Strahan, S. E., Sudo, K., and Szopa, S.: Multimodel ensemble simulations of present-day and near-future tropospheric ozone, J. Geophys. Res., 111, D08301, doi:10.1029/2005JD006338, 2006.

Stohl, A.: A 1 year Lagrangian "climatology" of airstreams in the Northern Hemisphere troposphere and lowermost stratosphere, J. Geophys. Res., 106, 7263, doi:10.1029/2000JD900570, 2001.

Stohl, A.: Intercontinental Transport of Air Pollution, The Handbook of Environmental Chemistry, Springer-Verlag, Berlin, Germany, 2004.

Stohl, A. and Trickl, T.: A textbook example of long-range transport: simultaneous observation of ozone maxima of stratospheric and North American origin in the free troposphere over Europe, J. Geophys. Res., 104, 30445, doi:10.1029/1999JD900803, 1999.

Stohl, A., Forster, C., Eckhardt, S., Spichtinger, N., Huntrieser, H., Heland, J., Schlager, H., Wilhelm, S., Arnold, F., and Cooper, O.: A backward modeling study of intercontinental pollution transport using aircraft measurements, J. Geophys. Res., 108, 4370, doi:10.1029/2002JD002862, 2003a.

ACPD
15, 23841–23891, 2015

Stohl, A., Wernli, H., James, P., Bourqui, M., Forster, C., Liniger, M. A., Seibert, P., and Sprenger, M.: A new perspective of stratosphere–troposphere exchange, B. Am. Meteorol. Soc., 84, 1565–1573, doi:10.1175/BAMS-84-11-1565, 2003b.
Stohl, A., Forster, C., Frank, A., Seibert, P., and Wotawa, G.: Technical note: The Lagrangian particle dispersion model FLEXPART version 6.2, Atmos. Chem. Phys., 5, 2461–2474, doi:10.5194/acp-5-2461-2005, 2005.
Struzewska, J. and Kaminski, J. W.: Formation and transport of photooxidants over Europe during the July 2006 heat wave – observations and GEM-AQ model simulations, Atmos. Chem. Phys., 8, 721–736, doi:10.5194/acp-8-721-2008, 2008.
Sudo, K. and Akimoto, H.: Global source attribution of tropospheric ozone: long-range transport from various source regions, J. Geophys. Res., 112, D12302, doi:10.1029/2006JD007992, 2007.
Tang, Q., Prather, M. J., and Hsu, J.: Stratosphere–troposphere exchange ozone flux related to deep convection, Geophys. Res. Lett., 38, L03806, doi:10.1029/2010GL046039, 2011.
Thouret, V., Marenco, A., Logan, J. A., Nédélec, P., and Grouhel, C.: Comparisons of ozone measurements from the MOZAIC airborne program and the ozone sounding network at eight locations, J. Geophys. Res., 103, 25695, doi:10.1029/98JD02243, 1998.
Thouret, V., Cammas, J.-P., Sauvage, B., Athier, G., Zbinden, R., Nédélec, P., Simon, P., and Karcher, F.: Tropopause referenced ozone climatology and inter-annual variability (1994–2003) from the MOZAIC programme, Atmos. Chem. Phys., 6, 1033–1051, doi:10.5194/acp-6-1033-2006, 2006.
Tiao, G. C., Reinsel, G. C., Pedrick, J. H., Allenby, G. M., Mateer, C. L., Miller, A. J., and DeLuisi, J. J.: A statistical trend analysis of ozonesonde data, J. Geophys. Res., 91, 13121, doi:10.1029/JD091iD12p13121, 1986.
Tressol, M., Ordonez, C., Zbinden, R., Brioude, J., Thouret, V., Mari, C., Nedelec, P., Cammas, J.-P., Smit, H., Patz, H.-W., and Volz-Thomas, A.: Air pollution during the 2003 European heat wave as seen by MOZAIC airliners, Atmos. Chem. Phys., 8, 2133–2150, doi:10.5194/acp-8-2133-2008, 2008.
Van Dingenen, R., Dentener, F. J., Raes, F., Krol, M. C., Emberson, L., and Cofala, J.: The global impact of ozone on agricultural crop yields under current and future air quality legislation, Atmos. Environ., 43, 604–618, doi:10.1016/j.atmosenv.2008.10.033, 2009.
Wilson, R. C., Fleming, Z. L., Monks, P. S., Clain, G., Henne, S., Konovalov, I. B., Szopa, S., and Menut, L.: Have primary emission reduction measures reduced ozone across Europe?

ACPD
15, 23841–23891, 2015

An analysis of European rural background ozone trends 1996–2005, Atmos. Chem. Phys., 12, 437–454, doi:10.5194/acp-12-437-2012, 2012.

Worden, H. M., Deeter, M. N., Frankenberg, C., George, M., Nichitiu, F., Worden, J., Aben, I., Bowman, K. W., Clerbaux, C., Coheur, P. F., de Laat, A. T. J., Detweiler, R., Drummond, J. R., Edwards, D. P., Gille, J. C., Hurtmans, D., Luo, M., Martínez-Alonso, S., Massie, S., Pfister, G., and Warner, J. X.: Decadal record of satellite carbon monoxide observations, Atmos. Chem. Phys., 13, 837–850, doi:10.5194/acp-13-837-2013, 2013.

Wotawa, G., Novelli, P. C., Trainer, M., and Granier, C.: Inter-annual variability of summertime CO concentrations in the Northern Hemisphere explained by boreal forest fires in North America and Russia, Geophys. Res. Lett., 28, 4575–4578, doi:10.1029/2001GL013686, 2001.

Wu, S., Mickley, L. J., Jacob, D. J., Logan, J. A., Yantosca, R. M., and Rind, D.: Why are there large differences between models in global budgets of tropospheric ozone?, J. Geophys. Res., 112, D05302, doi:10.1029/2006JD007801, 2007.

Zbinden, R. M., Cammas, J.-P., Thouret, V., Nédélec, P., Karcher, F., and Simon, P.: Mid-latitude tropospheric ozone columns from the MOZAIC program: climatology and interannual variability, Atmos. Chem. Phys., 6, 1053–1073, doi:10.5194/acp-6-1053-2006, 2006.

Zbinden, R. M., Thouret, V., Ricaud, P., Carminati, F., Cammas, J.-P., and Nédélec, P.: Climatology of pure tropospheric profiles and column contents of ozone and carbon monoxide using MOZAIC in the mid-northern latitudes (24° N to 50° N) from 1994 to 2009, Atmos. Chem. Phys., 13, 12363–12388, doi:10.5194/acp-13-12363-2013, 2013.

ACPD
15, 23841–23891, 2015

Table 1. Annual and seasonal linear trends of mean ozone concentrations, 5th and 95th percentiles, and uncertainties at the 95 % confidence level. Trends with p value below 0.05 are indicated in bold.

Season	Layer	O_3 trend (ppb yr^{-1}) (1994–2012)			CO trend (ppb yr^{-1}) (2002–2012)		
		Mean	5th	95th	Mean	5th	95th
Year	UT	+0.22 ± 0.23	**+0.25 ± 0.20**	+0.10 ± 0.33	**−1.16 ± 0.88**	−0.70 ± 1.32	**−1.97 ± 1.11**
	MT	+0.13 ± 0.18	**+0.21 ± 0.15**	+0.10 ± 0.24	**−1.87 ± 0.92**	**−1.16 ± 1.12**	**−2.72 ± 1.02**
	LT	+0.11 ± 0.21	**+0.35 ± 0.15**	−0.27 ± 0.39	**−2.62 ± 1.22**	**−1.91 ± 1.40**	**−4.41 ± 1.34**
Winter	UT	**+0.36 ± 0.31**	**+0.41 ± 0.37**	**+0.51 ± 0.45**	**−1.96 ± 1.15**	**−1.56 ± 1.28**	**−2.49 ± 1.23**
	MT	**+0.31 ± 0.24**	**+0.32 ± 0.25**	**+0.30 ± 0.29**	**−2.04 ± 1.32**	**−1.42 ± 1.41**	**−2.30 ± 1.56**
	LT	**+0.38 ± 0.24**	**+0.43 ± 0.33**	**+0.42 ± 0.30**	−2.01 ± 2.33	−1.72 ± 1.92	−1.15 ± 6.35
Spring	UT	**+0.26 ± 0.30**	+0.26 ± 0.29	−0.13 ± 0.74	**−2.15 ± 1.23**	**−1.55 ± 1.22**	**−2.74 ± 1.81**
	MT	**+0.19 ± 0.22**	+0.18 ± 0.20	+0.21 ± 0.32	**−2.81 ± 1.49**	**−2.42 ± 1.84**	**−3.44 ± 1.65**
	LT	+0.14 ± 0.25	+0.25 ± 0.29	−0.09 ± 0.33	**−3.05 ± 1.60**	**−2.36 ± 1.99**	**−5.53 ± 2.95**
Summer	UT	+0.21 ± 0.31	+0.30 ± 0.30	+0.02 ± 0.45	−0.99 ± 1.21	−0.74 ± 1.54	**−1.62 ± 1.36**
	MT	−0.01 ± 0.23	+0.05 ± 0.20	+0.02 ± 0.42	**−1.72 ± 1.23**	−1.01 ± 1.26	**−2.98 ± 1.68**
	LT	−0.21 ± 0.34	+0.13 ± 0.27	−0.40 ± 0.51	**−3.06 ± 1.70**	**−2.18 ± 1.18**	**−4.54 ± 2.44**
Autumn	UT	+0.21 ± 0.25	**+0.32 ± 0.25**	−0.01 ± 0.46	−0.98 ± 1.67	−0.64 ± 1.49	−1.51 ± 2.04
	MT	**+0.19 ± 0.19**	**+0.28 ± 0.13**	+0.24 ± 0.25	−1.76 ± 2.02	−1.11 ± 1.32	−2.38 ± 2.72
	LT	**+0.29 ± 0.20**	**+0.47 ± 0.22**	**+0.38 ± 0.32**	−2.67 ± 2.87	−1.70 ± 2.20	**−5.54 ± 4.57**

ACPD
15, 23841–23891, 2015

Table 2. Informations about surface and ozonesonde stations.

	Location	Altitude
Surface stations		
Kollumerwaard (the Netherlands)	53.3° N, 6.3° E	0 m
Vindeln (Sweden)	64.2° N, 19.8° E	271 m
Kosetice (Czech Republic)	49.6° N, 15.1° E	534 m
Sonnblick (Austria)	47.0° N, 12.9° E	3106 m
Neuglobsow (Germany)	53.2° N, 13.0° E	65 m
Westerland (Germany)	54.9° N, 8.3° E	12 m
Schauinsland (Germany)	47.9° N, 7.9° E	1205 m
Zingst (Germany)	54.4° N, 12.7° E	1 m
Waldhof (Germany)	52.8° N, 10.8° E	74 m
Payern (Switzerland)	46.8° N, 7.0° E	490 m
Jungfraujoch (Switzerland)	46.5° N, 8.0° E	3580 m
Rigi (Italy)	46.1° N, 8.4° E	1031 m
Ozonesonde sites		
Hohenpeissenberg (Germany)	47.8° N, 11.0° E	960 m
De Bilt (the Netherlands)	52.1° N, 5.2° E	4 m
Uccle (Belgium)	50.8° N, 4.4° E	85 m

ACPD
15, 23841–23891, 2015

Table 3. Seasonal shifts between 1995–2004 and 2003–2012 at the three ozonesonde sites and for different pressure levels, and uncertainties at a 95 % confidence level. Negative values indicate a decreasing seasonlity phase (i.e. toward ealier O_3 maximum). Trends with p value below 0.05 are indicated in bold.

Pressure level	Seasonal shift (days decade^{-1})		
	Hohenpeissenberg	De Bilt	Uccle
300–400 hPa	**−3.8 ± 3.0**	−5.0 ± 6.2	**+7.5 ± 5.7**
400–600 hPa	**−2.9 ± 1.3**	**−4.8 ± 3.6**	−2.6 ± 4.6
600–800 hPa	**−6.7 ± 2.1**	**−15.9 ± 5.4**	**−11.6 ± 3.1**
800–900 hPa	**−5.1 ± 2.7**	**−17.5 ± 7.0**	**−20.1 ± 6.9**

ACPD
15, 23841–23891, 2015

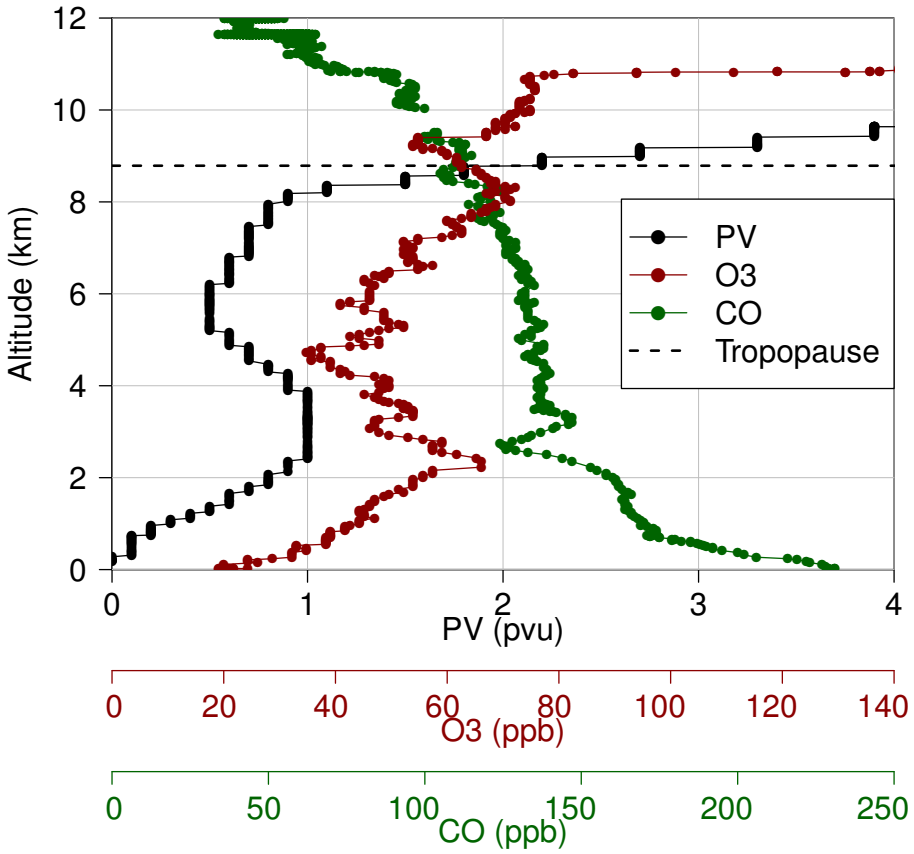

Figure 1. Vertical profile of potential vorticity (PV), O_3 and CO concentrations during the Frankfurt–Boston flight (19 March 2002) takeoff. The tropopause altitude (dotted black line) is estimated based on PV (see text for the methodology).

ACPD
15, 23841–23891, 2015

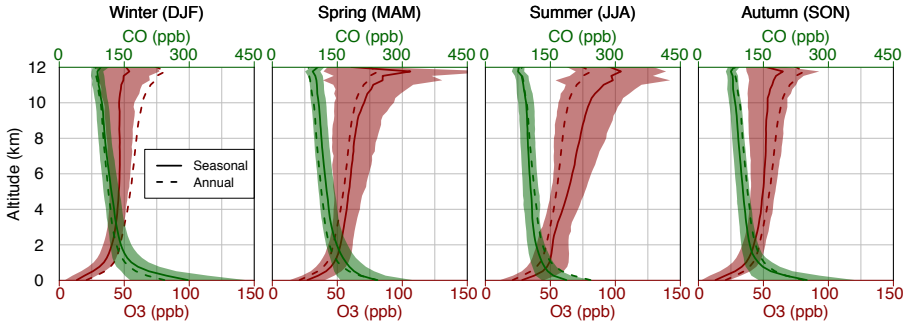

Figure 2. Climatological vertical profiles of ozone and carbon monoxide above Frankfurt per season (continuous lines). Standard deviation is also indicated (filled contour), as well as the overall climatological profile considering all seasons (dotted line).

ACPD
15, 23841–23891, 2015

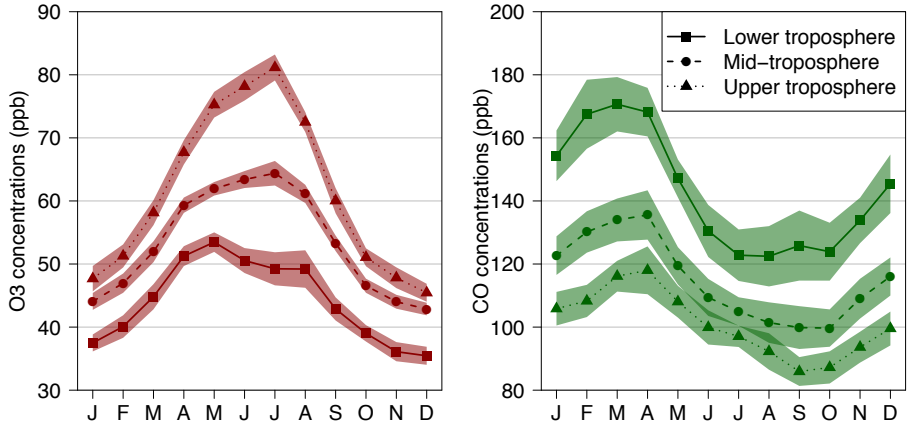

Figure 3. Averaged O_3 (left panel) and CO (right panel) monthly profiles above Frankfurt/Munich in the three tropospheric sublayers.

ACPD
15, 23841–23891, 2015

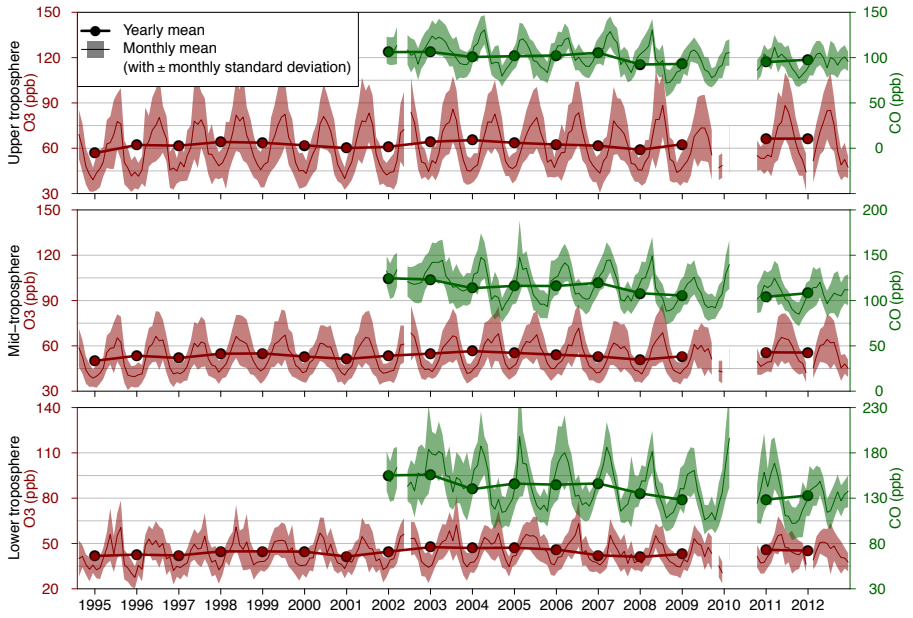

Figure 4. Monthly and yearly mean O_3 and CO concentrations of combined Frankfurt and Munich vertical profiles, in the lower (bottom panel), mid- (middle panel) and upper troposphere (top panel) between 1994 and 2012.

ACPD
15, 23841–23891, 2015

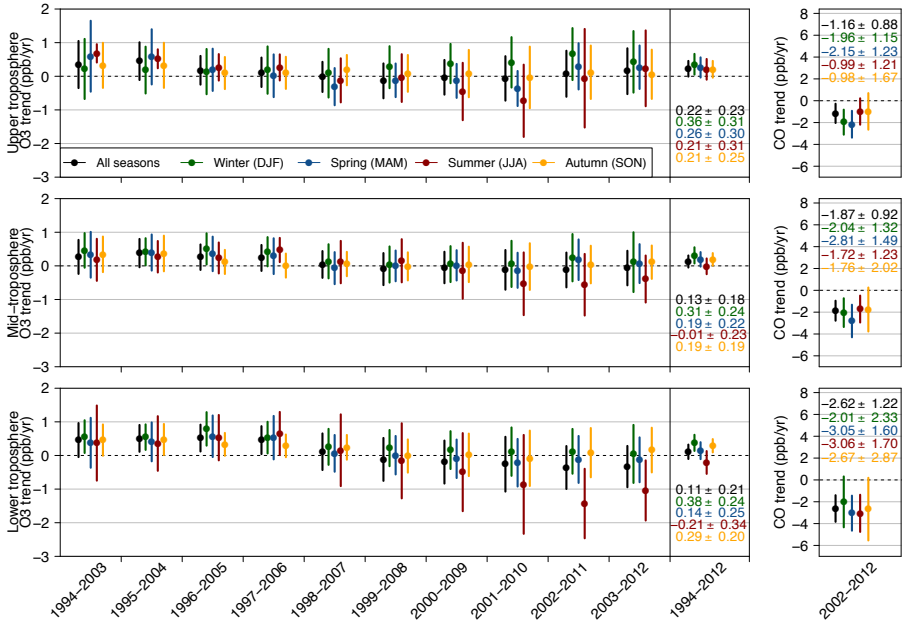

Figure 5. Annual and seasonal ozone (left panel) and CO (right panel) linear trends on moving 10-years periods (for ozone only) and along the whole period. Uncertainties (vertical bars) are indicated at the 95 % confidence interval. Trends and uncertainties over the 1994–2012 period are also indicated.

ACPD
15, 23841–23891, 2015

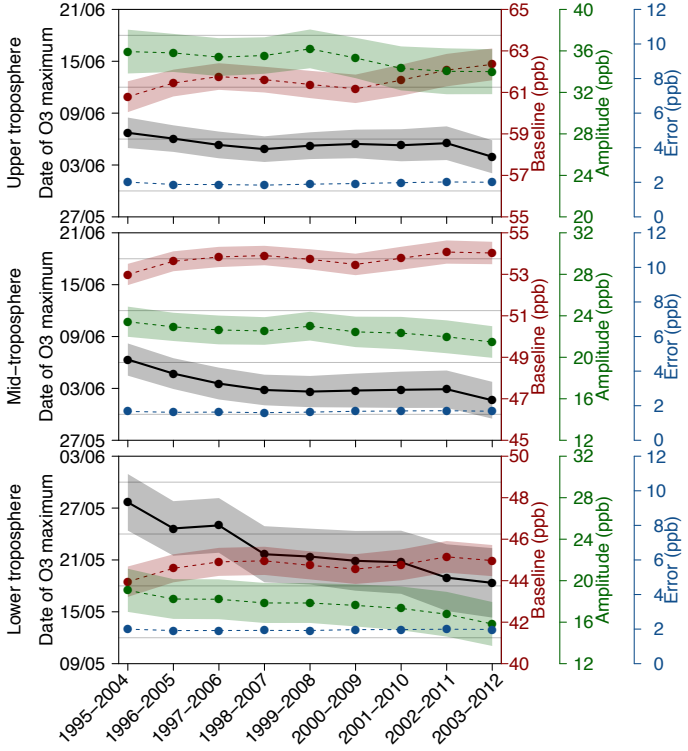

Figure 6. Date of O_3 maximum (in black), baseline (in red) and amplitude (in green) of the ozone seasonal cycle, and error (in blue) on moving periods of 10 years. For the three first parameters, 95 % confidence intervals are indicated. Layers: upper troposphere (top), mid-troposphere (middle), lower troposphere (bottom). Note that the same scale (but different offsets) is used for both the baseline and the amplitude in all sublayers, so that trends and confidence intervals are thus directly comparable.

ACPD
15, 23841–23891, 2015

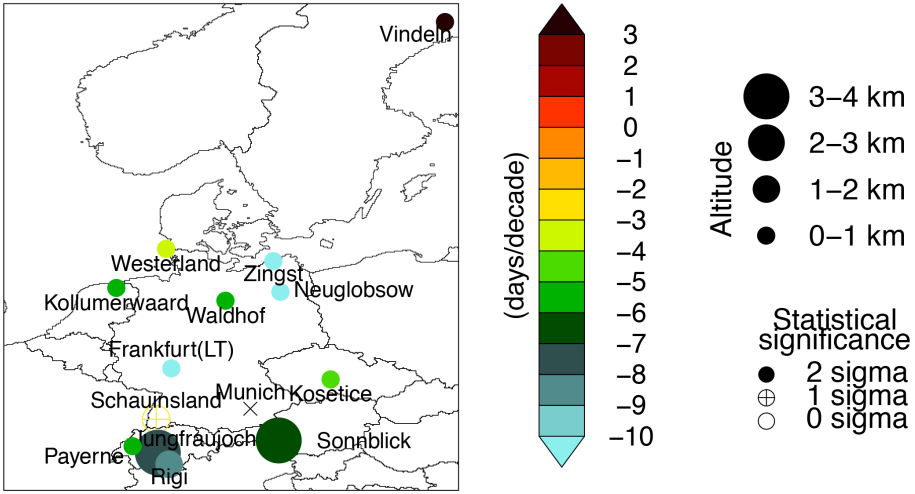

Figure 7. Phase shift trends over the 1994–2012 period at GAW monitoring sites (days decade^{-1}). Calculations are performed using the same procedure than for MOZAIC-IAGOS vertical profiles. Indications on the stations altitude and the statistical significance of trends are also given.

ACPD
15, 23841–23891, 2015

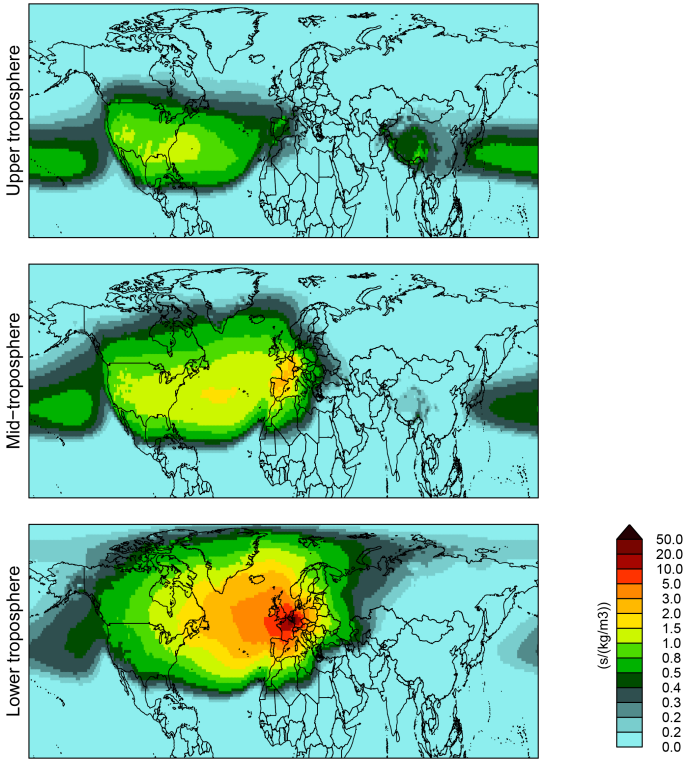

Figure 8. Average residence time (in the first kilometer) of air masses sampled in the three tropospheric sublayers around Frankfurt between 1994 and 2012. Note the irregular scale.

ACPD
15, 23841–23891, 2015

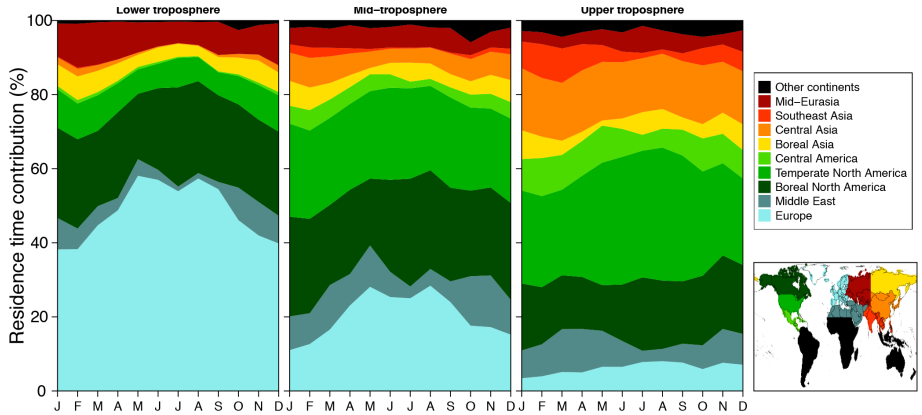

Figure 9. Averaged monthly profile of regional contributions to residence times (in the first kilometer) of air masses sampled in lower, mid- and upper troposphere over the 1994–2012 period.

ACPD
15, 23841–23891, 2015